Ph.D. dissertation 1981

NON-LINEAR CONDUCTION IN SUPERCONDUCTORS

B. D. Josephson

Dissertation submitted in application for the degree of
Doctor of Philosophy
at the University of Cambridge

Trinity College,
Cambridge.

August 1964.

PREFACE

The work described in this dissertation was carried out at the Royal Society Mond Laboratory, Cambridge. The dissertation is not substantially the same as any which I might have submitted for a degree or diploma or other qualification at any University other than that of Cambridge, and indeed no part of it has already, or is being concurrently, submitted for any such degree, diploma or other qualification.

Throughout the text, acknowledgement of the work of others has been made explicitly or by references. In part I, chapters 1 and 4 summarize the work carried out by others in the field and are essentially not original. The experiments described in chapters 2 and 3 are believed to be original as is also the application of the calculation of the appendix to chapter 3. Part II is an account of a field of research originated by the author and is nearly all original, except where results obtained by others working in the field have been quoted for completeness or for illustrative purposes. In such cases the fact that the result is not due to the present author is made clear in the text. It is, however, probably inevitable that in the expository parts of the work ideas picked up in conversation with others have been incorporated.

I am grateful to my supervisor, Professor A. B. Pippard, for suggesting the experiment described in Part I of the dissertation and for his ever ready advice on how to carry it out and overcome

the difficulties that arose; to Dr. P. W. Anderson for many stimulating discussions during his stay at Cambridge during the year 1961-2; to the workshop staff for the construction of the main parts of the apparatus and the supply of liquid helium, and for their helpful advice on matters of design and technique; and to the many other members of the staff and research students with whom I have had useful discussions on experimental and theoretical topics. I should also like to thank Trinity College for their generous financial support throughout the period of the research project, and the Department of Scientific and Industrial Research for providing partial financial support for the first two years.

B. D. Josephson

August 10th, 1964.

CONTENTS

Location of tables, diagrams and photographs

N.B. In this list * denotes 'opposite' and - denotes 'beneath'.

INTRODUCTION

Part I of this dissertation is concerned with the problem of the magnetic field dependence of the surface impedance of superconductors, with particular reference to tin. In chapter 1 the predictions of the simple theory for the behaviour of the surface impedance for different frequencies and field configurations are described and compared with the results of previous experiments. Chapter 2 deals with the experimental side of the present work, where a frequency of 170 Mc/s was used, and in chapter 3 the results obtained are discussed. In chapter 4 the attempts which have been made to account theoretically for the experimental observations are reviewed.

Part II of the dissertation is concerned with another problem in superconductivity, namely the behaviour of superconducting systems partitioned by thin barriers of substances which in bulk are not superconducting. The theory of such systems is developed, the consequences investigated in some detail and the present experimental situation reviewed.

Part I

FIELD DEPENDENCE OF THE SURFACE IMPEDANCE OF SUPERCONDUCTORS

Chapter 1. General background.

(i) The penetration depth

One of the most basic properties of superconductors is the Meissner effect, discovered in 1933 by Meissner and Ochsenfeld, who showed that pure superconductors in a magnetic field behave as if the magnetic induction $\underline{B}$ in their interior is zero. This observation suggested the question of how fast a magnetic field applied to the surface of a superconductor falls off with distance from the surface. An answer to this question was provided by the theory of F. and H. London (1935). This theory assumed the existence in a superconductor of 'superconducting electrons' which under the influence of an electric field accelerate freely without encountering resistive forces. The basic equation of the Londons' theory for superconductors in equilibrium is the following:

$$c\Lambda \operatorname{curl} \underline{J} + \underline{B} = 0 \qquad (1)$$

where $\Lambda = m/n_s e^2$, m, n_s and e being the mass, number density and charge respectively of the superconducting electrons. From (1) and Maxwell's equations can be deduced the penetration equation

$$\nabla^2 \underline{B} = \underline{B}/\lambda^2 \qquad (2)$$

which shows that $\underline{B}$ falls off exponentially with distance from the surface in a characteristic distance λ, the penetration depth, given by

$$\lambda = (mc^2/4\pi n_s e^2)^{\frac{1}{2}} \qquad (3)$$

In the general case when the Londons' equations may not be obeyed, it is convenient to define the penetration depth as

$$\lambda = \frac{\int_0^\infty H(z)dz}{H(0)} \qquad (4)$$

where H(z) is the field at a depth z below the surface. When the Londons' equations are valid, $H(z) = e^{-(z/\lambda)}H(0)$, so this definition reduces to the previous one.

(ii) Temperature dependence of the penetration depth

Originally the Londons identified n_s with n, the number density of conduction electrons, which occurs in the discussion of such normal state properties as the conductivity and the Hall effect. This predicted a penetration depth of the order of 10^{-6} cm. When measurements of the penetration depth were carried out it was found to be considerably greater, indicating that n_s is much smaller than n. Furthermore, it was found that as one approaches the transition temperature T_c the penetration depth tends to infinity, so that n_s tends to zero at T_c.

The Londons' theory may be combined with the two-fluid model of Gorter and Casimir (1934), according to which a superconductor consists of an equilibrium mixture of two fluids, composed of 'superconducting electrons' and 'normal electrons' respectively. n_s is then the number density of the superconducting component (alternatively it may be thought of as an order parameter, in the sense of the Landau theory of phase transitions (Landau and Lifshitz 1959)), and T_c is the point at which n_s becomes zero and the characteristic

superconducting properties disappear (through Λ becoming infinite).

(iii) Field dependence of the penetration depth.

It is to be expected that the proportion of superconducting electrons will be a function not only of temperature, as in section (ii), but also of magnetic field. We know in particular that application of fields greater than the critical field causes a superconductor to change into the normal state ($n_s = 0$). One would therefore expect that in fields less than the critical field n_s might be reduced in the penetration region, with a corresponding increase in the penetration depth.

A more sophisticated argument giving rise to the same conclusion is due to H. London (unpublished, see Pippard 1950), and is as follows. If we ignore the penetration region, and suppose that the specimen has such a shape that demagnetizing effects can be ignored, then the magnetization per unit volume of a superconductor, M, is $H/4\pi$, where H is the applied field. The effect of the finite distance of penetration of the field is to reduce M slightly. Since the penetration depth increases with temperature, it follows that $(\partial M/\partial T)_H$ is negative. By a Maxwell relation it follows that $(\partial S/\partial H)_T$ is positive, so that the entropy of the superconductor increases with H. This entropy increase is presumably associated with a decrease in n_s, since the entropy of the normal state ($n_s=0$) is known from specific heat measurements to be greater that that of the superconducting state ($n_s > 0$).

(iv) The Ginzburg-Landau theory

A theory which makes detailed predictions of the field dependence of the penetration depth is the Ginzburg-Landau theory (Ginzburg and Landau 1950). This differs from the two-fluid model in using a complex order parameter ψ. $|\psi|^2$ is proportional to n_s of the two-fluid model, and the appearance of an order parameter with phase as well as amplitude reflects the wave nature of the electron in quantum theory, which manifests itself on a macroscopic scale in superconductivity.

The Ginzburg-Landau theory (hereafter referred to as the G-L theory) proceeds by applying the variational principle to a suitable thermodynamic potential (Gibbs free energy). The main advance of the G-L theory is the inclusion of a term $\frac{1}{2m}\left|\left(-i\hbar\nabla-\frac{e^*}{c}A\right)\psi\right|^2$ containing the magnetic vector potential $\underline{A}$, where according to Gor'kov (1959) e* is twice the electronic charge. The equilibrium state of the system in the G-L theory is obtained by minimizing the Gibbs free energy with respect to variations of both ψ and A. Equations are then obtained from which the properties of a superconductor in a magnetic field can be deduced. In weak fields these reduce to the Londons' equations.

The G-L equations at a given temperature involve only two adjustable parameters, which can be determined from two experimental parameters such as the critical field H_c and the small field penetration depth $\lambda(0)$. From these may be derived the important

dimensionless quantity

$$\kappa = \sqrt{2}\,\frac{e^*}{\hbar c}\,H_c\,\lambda^2(0) \qquad (5)$$

Experiment shows that for pure tin $\kappa = 0.16$ (Lynton 1962). The G-L equations make the following predictions for the field dependence of λ (Ginzburg and Landau 1950, Sharvin and Gantmakher 1961):

$$\lambda(H) = \lambda(0)\{1 + \alpha(H/H_c)^2 + \beta(H/H_c)^4 + \ldots\ldots) \qquad (6)$$

where $$\alpha = \frac{\kappa(\kappa + 2\sqrt{2})}{8(\kappa + \sqrt{2})^2} \qquad (7)$$

and $$\beta = 0.047\,\kappa^2(1 - 5.1\kappa + 7\kappa^2) \qquad (8)$$

for $\kappa \ll 1$. For Sn, β is very small and the quadratic approximation for $\lambda(H)$ should be quite good for all fields up to the critical field. It should be noted in particular that since $\alpha > 0$ the increase in λ with increasing H expected from simplified arguments is confirmed by the G-L theory.

(v) The surface impedance

There exist no methods using only static fields capable of measuring the penetration depth of a superconductor with sufficient accuracy to give useful information about its field dependence, and generally methods using high frequency fields are employed. These measure a quantity known as the surface impedance, defined as the electric field at the surface divided by the total current crossing unit length of surface in a direction parallel to the electric field. These two quantities will in general not be in phase, so that the surface impedance Z is in general complex. Its

real and imaginary parts are known as the surface resistance R and surface reactance X respectively. The surface inductance L may be defined by the familiar relation $X = \omega L$, where ω is the angular frequency.

These quantities may be related to the penetration depth in the following way. Suppose that the surface of the specimen is in the xy plane, with the electric field and currents in the x direction and the magnetic field in the y direction. We have from the Maxwell relation $\text{curl } E = -\frac{1}{c}\frac{\partial B}{\partial t}$:

$$E_x(0) = -\frac{i\omega}{c}\int_0^\infty H_y(z)\,dz \qquad (9)$$

and from the relation $\text{curl } H = 4\pi j/c$ (ignoring displacement currents):

$$H_y(0) = -\frac{4\pi}{c}\int_0^\infty j_x(z)\,dz \qquad (10)$$

It follows from the definition of Z that

$$Z = \frac{E_x(0)}{\int_0^\infty j_x(z)\,dz} = \frac{-\frac{i\omega}{c}\int_0^\infty H_y(z)\,dz}{-\frac{c}{4\pi}H_y(0)} = 4\pi i\omega\lambda/c^2 \qquad (11)$$

where $\lambda = \dfrac{\int_0^\infty H_y(z)\,dz}{H_y(0)}$ as in (4), but the H_y may now be complex. In general λ will also be complex, though it is clear that in the limit $\omega \to 0$ it will simply reduce to the static penetration depth defined earlier. Clearly, then, measurements of the surface impedance at sufficiently low frequencies can be used to give information about the penetration depth.

(vi) Effects of non-linearity; the quasi-static limit

Experimentally a situation in which a small alternating magnetic

field is superimposed on a steady field is often used. If non-linearity is present the steady and alternating fields cannot be considered in isolation and the results of the preceding section must be modified. It should be noted in passing that from definition (4), a field-dependent penetration depth implies the existence of non-linearity. We shall, however, concern ourselves only with the case in which the alternating fields are so small that we need consider only quantities which are of first order in them (though quantities of higher order in the static fields will have to be taken into account), and ac surface impedance can be defined as usual.

In this section we shall consider only the quasi-static limit, in which the frequency of the alternating fields is assumed to be so low that the superconductor is at each instant in the equilibrium state corresponding to the particular magnetic field present at its surface at that instant.

Following Ginzburg and Landau (1950), we neglect anisotropy effects, so that λ may be written as a function of $H(0) \equiv H_0$, so that

$$\int_0^\infty \underline{H}(z)\, dz = \underline{H}_0\, \lambda(H_0) \qquad (12)$$

for quasi-static fields, λ being the field-dependent static penetration depth. For small variations $\delta \underline{H}_0$

$$\int_0^\infty \delta \underline{H}(z) dz = \lambda(H_0)\, \delta \underline{H}_0 + \underline{H}_0\, \lambda'(H_0)\, \delta H_0 \qquad (13)$$

(note the distinction between δH_0 and $\delta \underline{H}_0$, δH_0 being the change in the amplitude of H_0).

In the present case we may regard the oscillating component of the field as a small variation $\delta\underline{H}$. The surface impedance is then given by the following modification of (11):

$$Z = 4\pi i\omega\tilde{\lambda}/c^2 \qquad (11')$$

where now $$\tilde{\lambda} = \frac{\int_0^\infty \delta\underline{H}(z)\,dz}{\delta\underline{H}_0} \qquad (14)$$

Let us now consider two special cases: (i) $\delta\underline{H}_0 \perp \underline{H}_0$ and (ii) $\delta\underline{H}_0 \parallel \underline{H}_0$, which for experimental reasons are known as the longitudinal and transverse cases respectively. In the longitudinal case we have $\delta H_0 = 0$, and we obtain from (13) and (14) simply

$$\tilde{\lambda}(H_0) = \lambda(H_0) \quad \text{(longitudinal)} \qquad (15)$$

In the transverse case all magnetic fields lie in a fixed plane, so that (13) reduces to

$$\int_0^\infty \delta H(z)\,dz = (\lambda(H_0) + H_0\lambda'(H_0))\,\delta H_0$$

from which we deduce

$$\tilde{\lambda}(H_0) = \lambda(H_0) + H_0\lambda'(H_0) \quad \text{(transverse)} \qquad (16)$$

This formula is valid for any penetration law and assumes only isotropy and the quasi-static approximation. A more general relation can be derived if anisotropy is present.

A case of particular interest is when λ depends parabolically on H_0 (as will always be the case for small fields). Assuming

$$\lambda(H) = \lambda(0)\{1 + \alpha(H/H_c)^2\}$$

we have $$\lambda(H) + H\lambda'(H) = \lambda(0)\{1 + 3\alpha(H/H_c)^2\}$$

so that as pointed out by Ginzburg and Landau the field dependence of the surface impedance in the transverse case should be three times

as great as in the longitudinal case in the quasi-static limit. It should be noted that this derivation makes no assumptions as to the detailed form of the penetration law.

(vii) Frequency-dependent effects

This difference between the longitudinal and transverse cases in the quasi-static limit results from the fact that in the transverse case the fields are changing in magnitude and consequently the order parameter also changes. Naively one would expect that the change in the order parameter might be some kind of relaxation process, and that with increasing frequency the order parameter would become less able to follow the changes in magnitude of the field. At high frequencies the order parameter would not change at all and the surface impedance would be the same in a given static field whatever was the direction of the oscillating field. Thus $\delta Z_T/\delta Z_L$, the ratio between the field dependences in the transverse and longitudinal cases would change smoothly from 3 in the quasi-static limit to 1 at high frequencies.

(viii) Previous experimental results

The experimentally observed results on the field dependence of the surface reactance in superconducting tin are not at all in accordance with the simple picture derived in the last section. Observations have been made at various frequencies, 9.4 Gc/s by Pippard (1950), 3 Gc/s by Richards (1962), 1 Gc/s by Spiewak (1959) and 2 Mc/s by Sharvin and Gantmakher (1961).

Sharvin and Gantmakher observed values of δZ in fair agreement with the G-L theory, and also a value of $\delta Z_T/\delta Z_L$ consistent with the quasi-static value of 3. The observations at higher frequencies have been summarized by Pippard (1961), essentially as follows:

(i) In the longitudinal case δX is normally positive at all temperatures, as in the quasi-static limit.

(ii) In the transverse case δX is positive for low temperatures (say below $0{,}7\ T_c$). Close to T_c δX is negative at the lower frequencies and becomes positive as the frequency is increased.

It follows that at moderately high frequencies and close to T_c, $\delta X_T/\delta X_L$ may actually be negative, showing that our picture of the last section is considerably oversimplified. It is clear that a significant change in the behaviour of δX_T occurs between the frequencies 2 Mc/s and 1 Gc/s, and even for frequencies as low (compared, say, to the gap frequency) as 1 Gc/s the quasi-static approximation has broken down completely.

(ix) The present experiment

The object of the present experiment, suggested by Professor Pippard, was to start to fill in the previously mentioned gap in frequency, a factor of 500, between 2 Mc/s and 1 Gc/s. The frequency chosen was 170 Mc/s, and measurements were made of the field dependence of the surface reactance of superconducting tin over a wide range of temperatures in both the transverse and the longitudinal configurations.

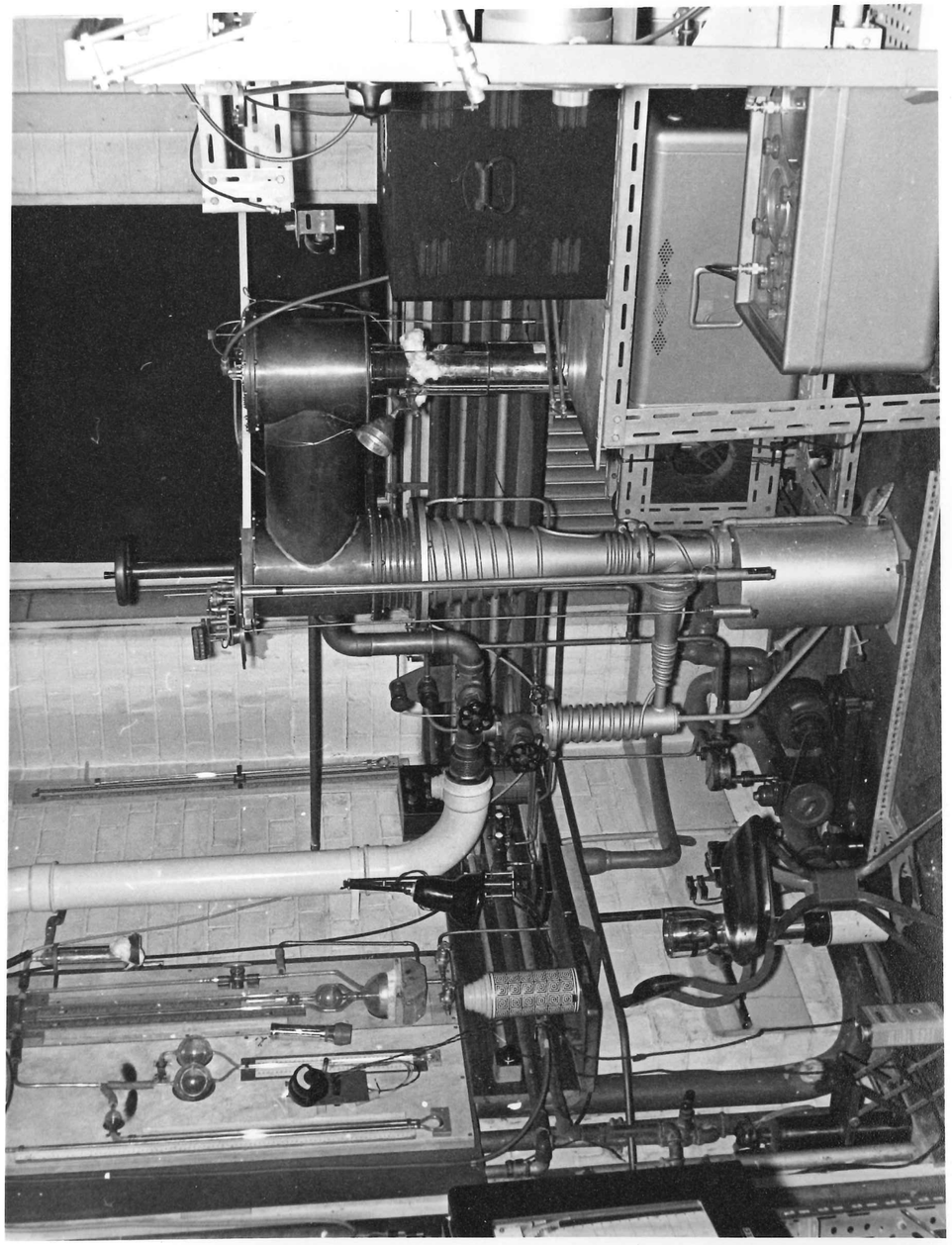

Fig. 1

Chapter 2. The experiment

(i) The resonance method

The essentials of the method employed to measure changes of surface impedance in the present experiment were suggested by Professor Pippard and are described in a paper by him (Pippard 1947). The basis of the method is to make a specimen of the substance under investigation in such a way that it will resonate electromagnetically at the frequency of interest (typically the specimen might be in the form of a resonant transmission line). Changes in the surface impedance of the specimen affect the boundary conditions satisfied by the electromagnetic field at its surface and hence its resonant frequency. More precisely, an increase in the surface reactance (assumed inductive) decreases the resonant frequency and an increase in the surface resistance decreases the Q of the resonance. Assuming that there are no other important resonances nearby and that the fractional frequency change is small, the change in frequency can be taken as proportional to the change in surface reactance.

In order to make the sensitivity of the method as great as possible the specimen must be in the form of a wire. In fact the fractional change in frequency is then of the order of the change in penetration depth divided by the diameter of the wire, so the diameter of the wire must be as small as possible. Its length is governed by the fact that the lowest frequency resonance of a conductor has a free space wavelength of the order of twice its

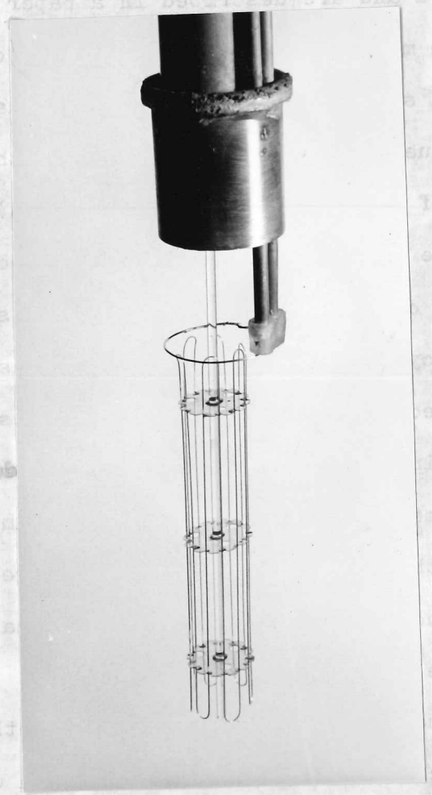

Fig. 2

greatest linear dimension.

(ii) The transmission method for determining resonant frequency

The resonant frequency was determined by the transmission method, the details of which can be seen from the photograph of fig. 2. The specimen is held inside a metal can into which two transmission lines go (in the photograph the can is removed to show details of the interior). The outer conductors of the transmission lines are connected to each other directly via the top of the can, and the inner conductors are joined by a loop of wire inside the can. An oscillator is connected to one transmission line and a matched detector to the other, the matching being adjusted so that in the absence of the specimen all the power is transmitted to the detector and none reflected back to the oscillator. When the specimen is in position and the oscillator is near the resonant frequency the specimen is set into oscillation, and some power is absorbed and some reflected, so that the power transmitted to the detector drops. An attenuator is placed between the oscillator and the specimen to prevent the oscillator being pulled by the reflected wave. In the ideal case a symmetrical resonance curve of power transmitted against frequency is obtained, but if the matching is not perfect an unsymmetrical resonance curve is obtained in general. Changes in the surface reactance will to a good approximation merely displace the whole resonance curve in frequency, if as in the present instance the frequency is so low that most of the losses are due to causes

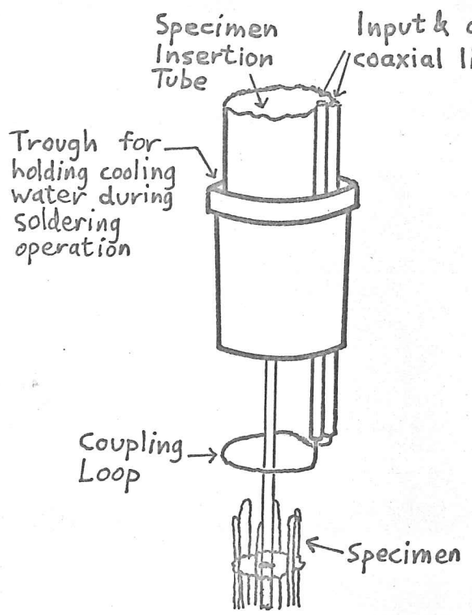

Fig. 3

other than the specimen. The effects of small changes in Q can be partly eliminated by the observational technique described later (section vi).

(iii) The apparatus 1: the cryostat

The details of the cryostat design were worked out in conjunction with Professor Pippard and Mr. F. Sadler, and the construction was carried out by Mr. W. Undrill of the Mond Laboratory workshop. The essential parts are the two transmission lines for carrying the rf signal, the specimen holder, and a screening can to prevent loss of power from the specimen by radiation and to allow the specimen to be at a different pressure from the helium bath. In addition a tube was provided to allow specimens to be inserted from the top of the cryostat, which also allowed the separation between the specimen and the coupling loop to be varied during an experiment. The design of the lower part of the cryostat can be seen from the photograph (fig 2), and the diagram of fig. 3. The coaxial lines each consisted of a 3mm. O.D. copper-nickel tube outer conductor and an inner conductor of 26 S.W.G. Eureka wire. The wire was supported in the tube by some of the polythene insulator obtained from a commercial coaxial cable. The polythene was cut up into short lengths to avoid difficulties due to contraction and was threaded on to the wire before being inserted into the tube. The polythene was prevented from falling out at the bottom by a piece of polystyrene, which also served to support the inner conductor. The two lines were made separately and the inner wires soldered

together afterwards to make the coupling loop. At the top of each transmission line was a socket which would accept a standard G.E.C. plug; this was a design of Mr. Sadler's using a tapered PTFE washer as a vacuum seal. The tube for inserting the specimen was an 18 mm. O.D. copper-nickel tube. The specimen was held on the end of a long 5 mm. tube which at the top end passed through an O-ring seal and at the bottom end had attached two sets of brass spring fingers which bore against the inside of the 18 mm. tube. At the bottom of the tube holding the specimen was inserted a short length of copper wire, which could be bent in order to align the specimen correctly for insertion in the tube (a system invented by Chambers (unpublished)). The screening can was made from 30 mm. O.D. copper-nickel tube electroplated on the inside with copper to reduce resistive losses. The coaxial lines and the specimen insertion tube were soldered into a brass top plate, which rested via an O-ring seal on top of an assembly which could be connected to the laboratory vacuum line, a booster pump, a small rotary pump, or the helium return line (fig. 1). Provision was made for pumping the specimen space and for filling the specimen space with helium from the helium bath. The pressure in the specimen space could be read with a mercury manometer and the bath pressure by either a mercury manometer, a differential oil gauge or a McLeod gauge. Specimen temperatures were obtained from the bath pressure, an estimated hydrostatic correction of 0.45 mm. of mercury being added to those obtained above the lambda-point.

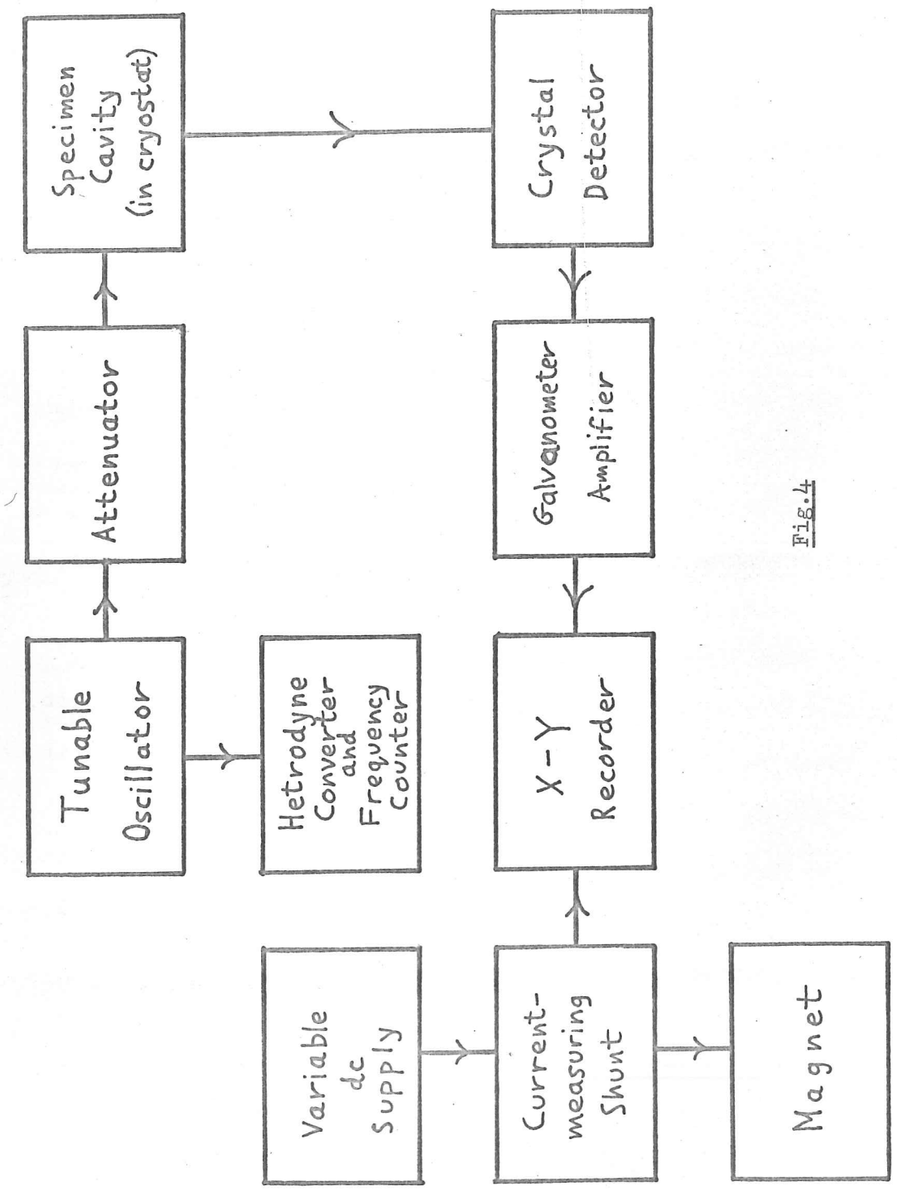

Fig.4

All soldered joints near the specimen had to be made of non-superconducting solder to avoid interference with the magnetic field. Hard solder was used for all joints except that holding the screening can, which it was forseen might have to be removed later. For this joint a zinc-cadmium alloy was used as solder. To avoid damage to the coaxial lines while this joint was being made, a trough which could be filled with cooling water was incorporated into the design and the heating was done electrically.

Thermal contact between the specimen and the helium bath was obtained by admitting into the specimen volume 1 cm. pressure of helium before cooling. The helium bath was contained in a glass Dewar surrounded by a liquid nitrogen shield. A temperature of 0.8 ^{o}K could be reached using the booster pump.

(iv) The apparatus 2: external circuitry.

The experimental arrangement in its final form is shown in the block diagram, fig. 4. In this section the arrangement used initially will be described.

Much of the equipment was that used previously for penetration depth measurements by McLean. We refer to McLean (1960) for fuller details not given here. The rf signal was generated by a triode oscillator constructed by McLean using a CV 273 triode with coaxial lines shorted by movable spring fingers as the frequency determining resonant elements. Coarse control of the frequency could be obtained by moving the spring fingers, while fine control could be obtained

by inserting metal or silica rods into the resonant line. The output was taken from one of the lines by variable capacitative coupling. The filament voltage was obtained from an accumulator and the HT supply from a stabilized power pack. Two-stage RC and LC filters of standard design in a screening can were used to prevent trouble due to power getting back along the supply lines. By careful setting of all the controls (grid voltage, feedback, length of coaxial lines) it was possible to get the oscillator to oscillate stably at the required frequency, with a drift which settled down eventually to a value of the order of 5 cycles/sec^2.

The frequency of the output was measured by a Beckmann/Berkeley pulse counter model 7370 together with a model 7572 hetrodyne frequency converter, which together displayed the output in digital form. Both models were controlled by the same thermostatically controlled crystal oscillator with a stability of $\pm$ 3x10^{-7} per week.

The oscillator was connected to the input line of the cryostat by attenuating cable, which was also used between the oscillator and the frequency meter, the object in both cases being to prevent reflected signals.

The output from the cryostat was taken to an adjustable matching device and then to a rectifier consisting of a point-contact diode inserted in the inner conductor of the transmission line. The output from the rectifier was then taken, in the preliminary experiments, to a galvanometer.

A pair of Helmholtz coils was mounted on a Dexion framework

to provide horizontal (transverse) magnetic fields and a solenoid was used to provide vertical (longitudinal) fields. The field distributions were measured and found to vary by less than 5% over the specimen region. Each magnet had a resistance of the order of an ohm. The magnets were powered by a 25 volt battery supply and the current was controlled by series rheostats. In the preliminary experiments, the current was measured directly by a sub-standard ammeter. The earth's field was not conpensated.

(v) Specimen preparation

As mentioned in section (i), the specimen must be in the form of a thin wire about half a wavelength long, or in the present case about 90 cm. The only suitable method for making and supporting wires of the necessary thinness is to cast them into fused silica capillary tubes and to leave them in the tubes during the experiment. Silica is suitable for this purpose because of its low electromagnetic losses and because tin contracts more than silica on cooling and does not stick to it, so that specimens prepared in this way have surface properties similar to those of unsupported specimens, as shown by Pippard (1950).

The first problem was to make capillaries of sufficient length. Capillaries are normally made by heating ordinary tubing in a flame while holding both ends till the viscosity of the quartz becomes very low, removing it from the flame and pulling sharply. The length of capillary required in the present case prevented this method on account of two factors, the length of the experimenter's

arms and the length to which the tube could be pulled before it got too cool to be stretched any further. The following method of making capillaries was accordingly devised. The top of the tube was held vertically in a clamp at a height of about six feet, and a weight of about $\frac{1}{2}$ kg. was clamped to the bottom of the tube, leaving a gap of a few centimetres in between. To heat up the necessary volume of silica an oxy-acetylene torch fitted with a jet of size no. 10 or larger was used. This was directed at the region between the clamps while the weight at the bottom was held in the free hand. When the silica was almost molten the flame was removed and the weight immediately released and allowed to fall into a bucket of sand, drawing out the tube into a capillary in the process. Some practice was necessary to get suitable results; if an insufficiently hot flame was used the weight would not fall far enough, and if an insufficiently great region was heated up the resulting capillary would have an extremely fine bore, though there seemed to be no danger of the tube closing up completely. By this method capillaries of length about 130 cm. and bore of the order of 0.1 mm. could be made.

The long capillaries then had to be bent to a suitable compact shape which would go into the cryostat. An important factor in determining the shape was the necessity of being able to separate out the longitudinal and transverse field cases. Since the currents flow along the axis of the wire the rf field is transverse to the wire, so that the longitudinal and transverse field cases defined

in chapter 1 actually correspond to steady fields longitudinal and transverse to the wire in this case. Professor Pippard drew attention to a paper by Tapp (1932) describing a method for making helices from silica fibres. With a helical wire of small pitch angle the more interesting transverse field case can be realized approximately when the steady field is parallel to the axis of the helix, while with the field at right angles to the axis the field will be transverse in some places, longitudinal in others and in between the field will have components in both directions.

Attempts were made to apply the Tapp method to the production of helical capillaries. Essentially the principle was to wind the capillaries on to a graphite rod with a small flame playing on the point where the capillary first made contact with the rod, in order to bend the capillary. A minature oxy-coal gas burner was made for this purpose. The rod was caused to move along its axis as it rotated by attaching it to a threaded rod rotating in a fixed mount. The capillary was guided in its approach to the rod by two slots and tensioned by friction or gravity. The main difficulty with this method was that the capillary tended to bend in polygons rather than smooth curves, and to become very fragile at the corners of the polygons. The maximum number of turns obtained by this method before the capillary stretched and snapped or met some other disaster was about ten, and was generally less. This was less than half of the length required, and various modifications tried met with no greater success.

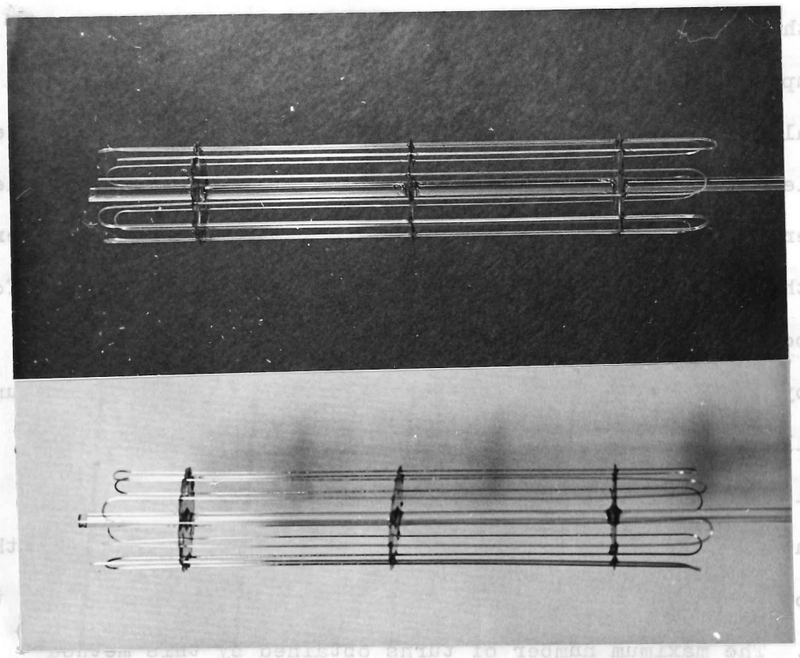

Fig. 5 Specimens before and after being filled with tin

In view of the difficulties involved in this method it was decided to leave the helical geometry for the time being and try a different one. This was essentially a zig-zag shape bent into a cylinder, and one such specimen can be seen in fig. 5. The production of such a shape involved only making a number of 180° bends in the capillary. One advantage of this shape is that apart from the bends all the wire is in one direction only, so that the transverse and longitudinal field cases can be investigated separately. However, there is the disadvantage that the length of the zig-zag needs to be considerably greater than half the free space wavelength at the resonant frequency. The reason for this is that adjacent sections of the zig-zag carry currents in opposite directions, which tends to decrease the magnetic energy for given currents and hence the self-inductance, while they carry charges of the same sign, which increases the electrostatic energy for given charge distribution and hence decreases the self-capacitance. The net effect is that the resonant frequency for a specimen of given length is increased. Estimates were made of the magnitude of this effect by using the variational principle to determine the frequency of resonance.

If we assume the current distribution along the wire in a normal mode to be $j(x)$ then the charge distribution (out of phase by $\pi/2$) is given by the continuity equation to be $\omega^{-1} \frac{dj}{dx}$, ω being the frequency of the mode. At one point in the cycle the energy is entirely magnetic, the current being at its peak, and a quarter of a cycle later the energy is entirely electrostatic, the charge density being

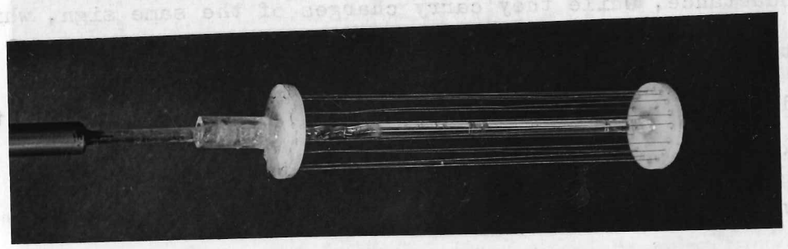

Fig. 6 Test specimen made from Nb wire

being at its maximum. Equating the two energies gives an expression for ω^2 in terms of j(x), and the variational principle tells us that the frequency and current distribution of the normal mode of lowest frequency can be found by choosing j(x) so as to minimize ω^2. In the present case the energies were calculated by treating the sections of the zig-zag as infinitely long, each one carrying a uniform charge density or current. For j(x) was assumed a Fourier series containing terms up to the fourth order, all except two vanishing by symmetry. The effect of the screening can was taken into account by the method of images.

The calculation showed that increases in length of the order of 50% would be required to make a specimen of the same resonant frequency as one which was half a free space wavelength long. The length would of course depend to a small extent on the diameter of the specimen and the number of sections of the zig-zag. To check this prediction a test specimen (fig. 6) was made up from some 0.005" niobium wire kindly provided by Dr. B. Abrahams. The wire was threaded through holes in two PTFE discs on a silica rod and held at the ends with araldite. The resonant frequency, measured in a liquid helium run, was about 10% less than the predicted value.

In deciding the length of capillary to be used for the real specimen to give the required resonant frequency, allowance was made for the dielectric nature of the silica, and on the strength of the result obtained with the test specimen a length of about 105 cm, was decided on. It was also decided to make the specimen with 12

sections of zig-zag, this being a compromise between the necessity of keeping the specimen short so that it should be in a fairly homogeneous field, and the difficulty of making a specimen with a larger number of sections.

The silica capillary was supported in triangular slots on the edge of three mica discs of diameter 15 mm, spaced 3 cm. apart on a 2 mm. silica rod, allowing just over 1 mm. clearance in the specimen insertion tube. Before the discs were attached to the rod one end of the rod was enlarged by heating in a flame and the other end inserted into a brass sleeve just large enough to take the main part of the rod. A 6 BA threaded rod was then screwed into the sleeve and held by a locknut. When the specimen had been made the silica rod was held firmly in the sleeve with black wax and the threaded rod used to attach the specimen to the specimen holder.

The adhesive used for attaching the mica discs to the central rod and the capillary to the mica discs was araldite I. This had two advantages compared to the usual two-tube form. In the first place it is better able to withstand the temperatures involved in filling the capillaries with molten tin. Secondly, as will be seen, its method of application made it possible to cure all the 36 joints together instead of separately as would have been necessary using two-tube araldite.

In the first attempts to make zig-zag specimens flat zig-zags were first made, using the minature flame to make the bends. This

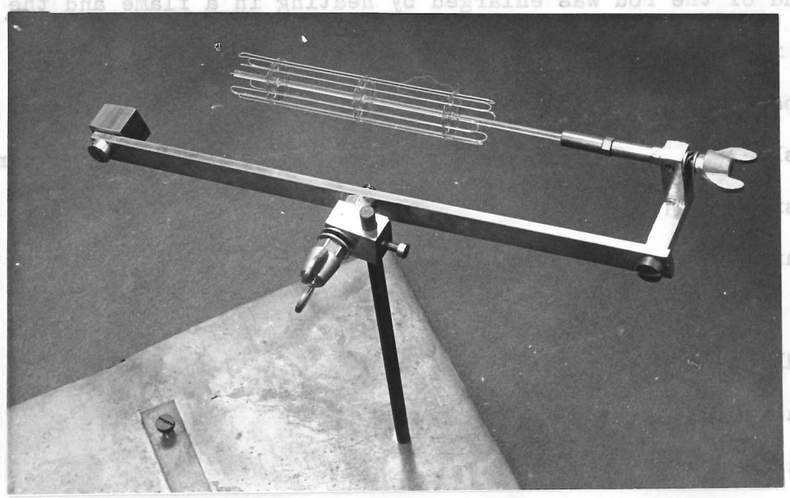

Fig. 7 Jig for making specimens

operation proved to be fairly straightforward, but difficulty was experienced making the zig-zag lie on the surface of a cylinder while sticking it into the slots on the mica discs. It was then realized that it would be much simpler to do the bending and sticking operations in a single operation. To facilitate the operation a jig was constructed (fig. 7) which allowed the specimen to be rotated about its axis and about a line at right angles to the axis. It should be explained at this point that araldite I is a wax-like solid with a low melting point, which is cured by heating. Since the adhesive is solid at room temperature the joints have a certain amount of strength even before the adhesive is cured, although of course the adhesive becomes liquid again when it is heated for the curing process.

The specimens were made in the following way. First the mica discs were stuck to the silica rod and the joints cured. The specimen was then placed in the jig and the capillary rested in the slots in the mica discs, and fixed temporarily with araldite I as described above, using a minature soldering iron run at reduced voltage to apply the adhesive. The capillary was then bent in the minature flame, the specimen being rotated so that gravity would cause the capillary to fall into the next set of slots. The capillary was then stuck to the next set of slots and the process continued as before.

When this process was finished the specimen was placed in an oven to cure the joints. The capillaries were held in the slots

during this process by wrapping fine wires round them, the wires being kept in tension by attaching weights to their ends.

The final step in preparing the specimens was to fill the capillaries with tin. In principle, the method was the following. One end of the capillary was sealed up. The capillary was evacuated and the open end immersed in molten tin. Nitrogen at atmospheric pressure was then used to force the molten tin into the capillary.

The experimental details were as follows. The tin used (Johnson Matthey spec. pure) was heated to red heat in a rotary pump vacuum to outgas it and reduce the danger of getting breaks due to bubbles in the column of tin in the capillary. The tin was bent into a ring and placed in the bottom of a metre long pyrex tube which had a small pip on the end to contain the tin after melting. The specimen was attached to a long rod going through a rubber bung at the top of the tube. The bung was also fitted with a tube for evacuating the system. A few inches of the open end of the capillary were left protruding beyond the specimen and, as suggested by Professor Pippard, the end was bent into such a shape as would prevent it being pulled against the side of the pyrex tube by the force due to the incoming tin.

The specimen having been positioned with the open end of the capillary in the pip, the tube was evacuated and clipped off. It was then placed vertically with its lower end in a furnace, which had been previously set to a temperature about 20°C above the melting point of tin. When the tin had melted and gone into the pip nitrogen was admitted into the tube. After allowing a few

minutes for the capillary to fill, the specimen was withdrawn slightly so that its end was clear of the tin, and the tube was removed from the furnace. At the first attempt a good specimen was obtained, all but about 1 cm. of the capillary being filled with a continuous length of tin. The protruding end of the specimen was broken off before the specimen was mounted.

(vi) The preliminary experiments and the consequent modifications

The first task was to find the resonant frequency of the specimen. This was originally done by using the fine tuning control of the oscillator and systematically covering the whole frequency range by setting the coarse controls suitably. The resonance showed itself as a sharp drop in output on the galvanometer. This process took a few hours, but was later speeded up by using a Marconi signal generator no. TF 801D/1 lent by Dr. Dobbs as the oscillator. This could be tuned through the frequency range in a few minutes without the output power fluctuating violently as would have happened using the coarse control on the McLean oscillator. To make the detector fast enough to respond to the sudden change in output on going through the resonance, the attenuating cable was dispensed with, thus making the output large enough to be detected on an oscilloscope.

Trouble was experienced at the beginning due to short circuits in the transmission lines down to the cryostat. This was traced to damage caused to the polythene and polystyrene during the operation of soldering on the screening can. This difficulty was overcome by replacing the polythene in the relevant parts by pyrex

and the polystyrene by araldite.

The method of measuring changes in resonant frequency of the sample was the following. The changes of resonant frequency on applying a magnetic field were so small (usually less than 1 kc/s or about 1% of the width of the resonance) as to make it unsatisfactory to proceed by plotting out complete resonance curves. Instead, the oscillator was set to a frequency on one side of the resonance, and the magnetic field switched on and off several times while noting down the galvanometer deflection, if necessary adjusting the oscillator tuning control to compensate for drift. These amplitude changes were then related to changes in resonant frequency by plotting a resonance curve at fixed magnetic field. To allow for possible changes in surface resistance the measurements were repeated on the other side of the resonance curve. Changes in surface resistance produce contributions of opposite sign in the two cases, and so averaging will largely eliminate the effects, in any case small, of surface resistance changes.

One disadvantage of the cryostat design manifested itself when the resonance had been found; the galvanometer spot showed violent jerky, irregular movements about the scale, making it difficult to estimate what to take as its mean position. This effect only occurred on resonance, indicating that it was due to fluctuations in resonant frequency, presumably due to motion of the specimen relative to the screening can. This effect was enhanced by the eccentric position of the specimen in the screening

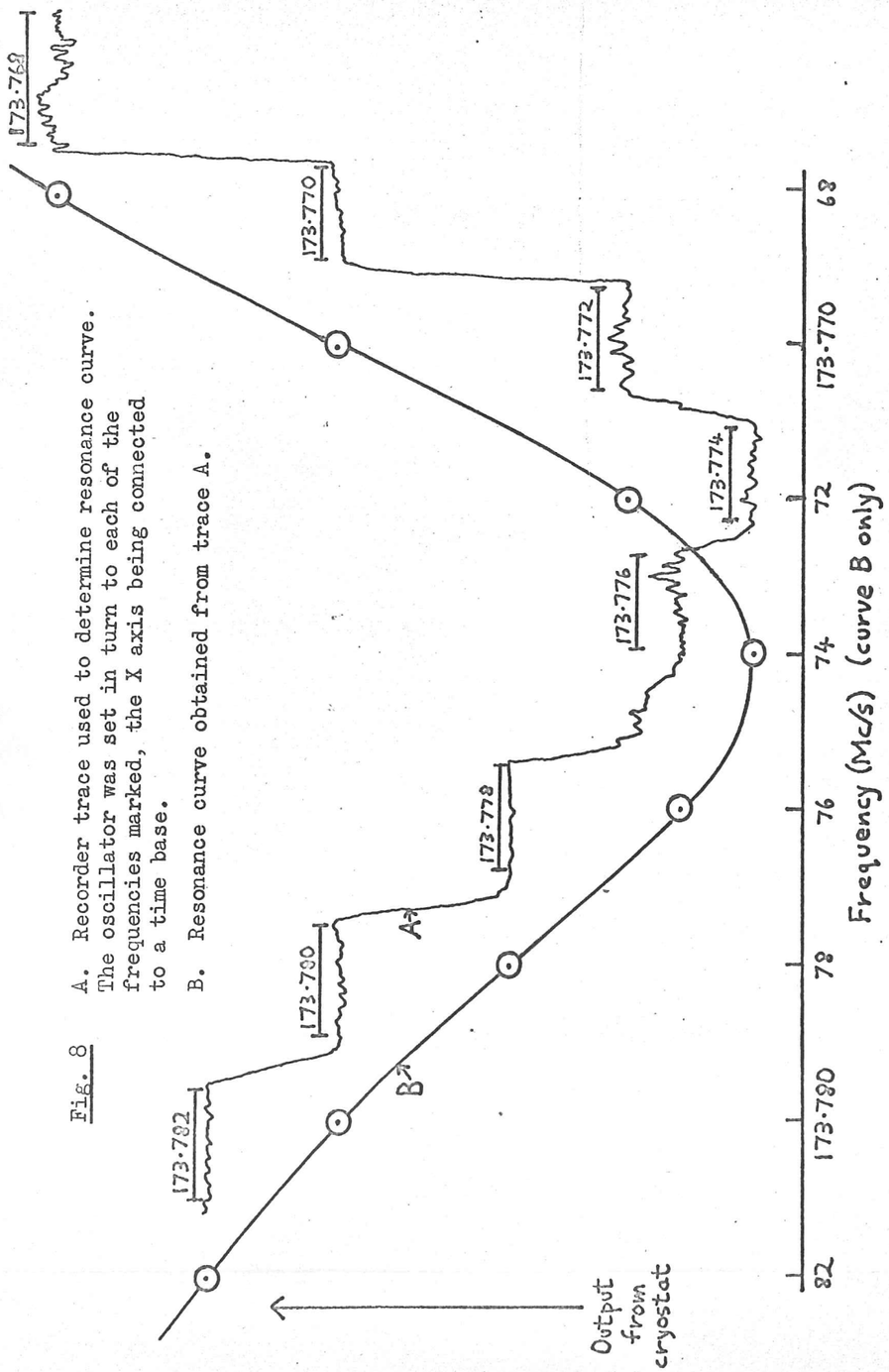

Fig. 8 A. Recorder trace used to determine resonance curve. The oscillator was set in turn to each of the frequencies marked, the X axis being connected to a time base.

B. Resonance curve obtained from trace A.

can and by the lack of symmetry of the specimen about its axis (since the ends of the capillary define a preferred direction). These assymmetries allow changes of frequency which are first order in the displacement. The largest bursts of activity, corresponding to frequency changes of some kilocycles per second, could be clearly identified with events such as slamming doors in the vicinity, people walking in the corridor or noisy machines being used in the construction of the new practical classes nearby. The other troublesome disturbances were probably due to similar causes of intensity too small to be noticed by other means, rather than to the boiling of the nitrogen or the vibrations of the pump, which would have caused effects similar to random noise.

The exact way in which vibrations affected the output power did not become clear until the output was plotted on a pen recorder (figs. 8,9). It will be seen from these traces that the disturbances tend to be in one direction only, and that their magnitude and sign vary in a similar manner to the second derivative of the amplitude with respect to frequency. This indicates that the measuring device is not responding to the fast vibrations of the specimen, but is acting as a square law detector, owing to the non-linearity of the amplitude-frequency curve. Therefore the noise can be reduced by working near the point of inflexion of the resonance curve, and by broadening the resonance curve by coupling the specimen more strongly.

The effects of the external vibrations could probably have been made negligible if the specimen could have been fixed rigidly against the screening can. However, this was not very feasible with the present design, adopted to avoid the necessity of frequent soldering and unsoldering of the screening can, in which the specimen was inserted from the top of the cryostat. Failing this, various other devices were tried to reduce the vibration of the specimen. The screening can was supported in the helium dewar by spring fingers. The copper wire link to the specimen mentioned in section (iii) was stiffened with araldite once it had been bent into the correct position, and the effect of replacing the spring fingers supporting the specimen in the specimen insertion tube by a kinematic slide was noted but found to be negligible. A device invented by Preston-Thomas (1949) to prevent the nitrogen bubbling was made, but this was not very successful since it tended to block up when the nitrogen evaporated after a run. Finally, the only measure which had any significant effect was to work at night. Apart from the period when the porter made his nightly tour of the laboratory, there were few large disturbances then.

Improvements were also made to the detection side of the experiment. A twin-channel recording milliammeter was used to record the information obtained, and allow a less subjective separation of the signal from the noise. Into one channel was fed the output signal amplified by a galvanometer amplifier. A filter was placed between the crystal detector and the amplifier, just

as was used in the power supply to the oscillator, to prevent variable amounts of rf power being reflected back from the amplifier to the detector. To the other channel was connected a signal derived from the magnet current. The recorder was oil damped with a time constant of a few seconds. Readings were taken as before by switching the magnet on and off several times. Some trouble was had near the transition temperature owing to drifts in temperature of the bath, so an Adkins temperature stabilizer (Adkins 1961) was fitted. This type of stabilizer detects changes in the bath temperature by means of a differental oil manometer, and controls the temperature by altering the current through a heater at the bottom of the cryostat.

A few observations were made by this method, but it was soon decided to replace the recording milliammeter by a Moseley servo-controlled X-Y recorder. One advantage of doing this was that the whole behaviour of penetration depth as a function of field could be displayed by varying the field with the rheostats while plotting output power directly against magnet current. The signal corresponding to the magnet current was in this case obtained from the voltage developed across a shunt in series with the magnet. Further, the X-Y recorder had such a fast response time that it was possible to draw complete plots in between major disturbances affecting the specimen. It was also possible to compensate for the component of the earth's field in the direction of the magnet's field by plotting the behaviour with both directions of field and making use of the symmetry of the curve to find the point corresponding to zero total

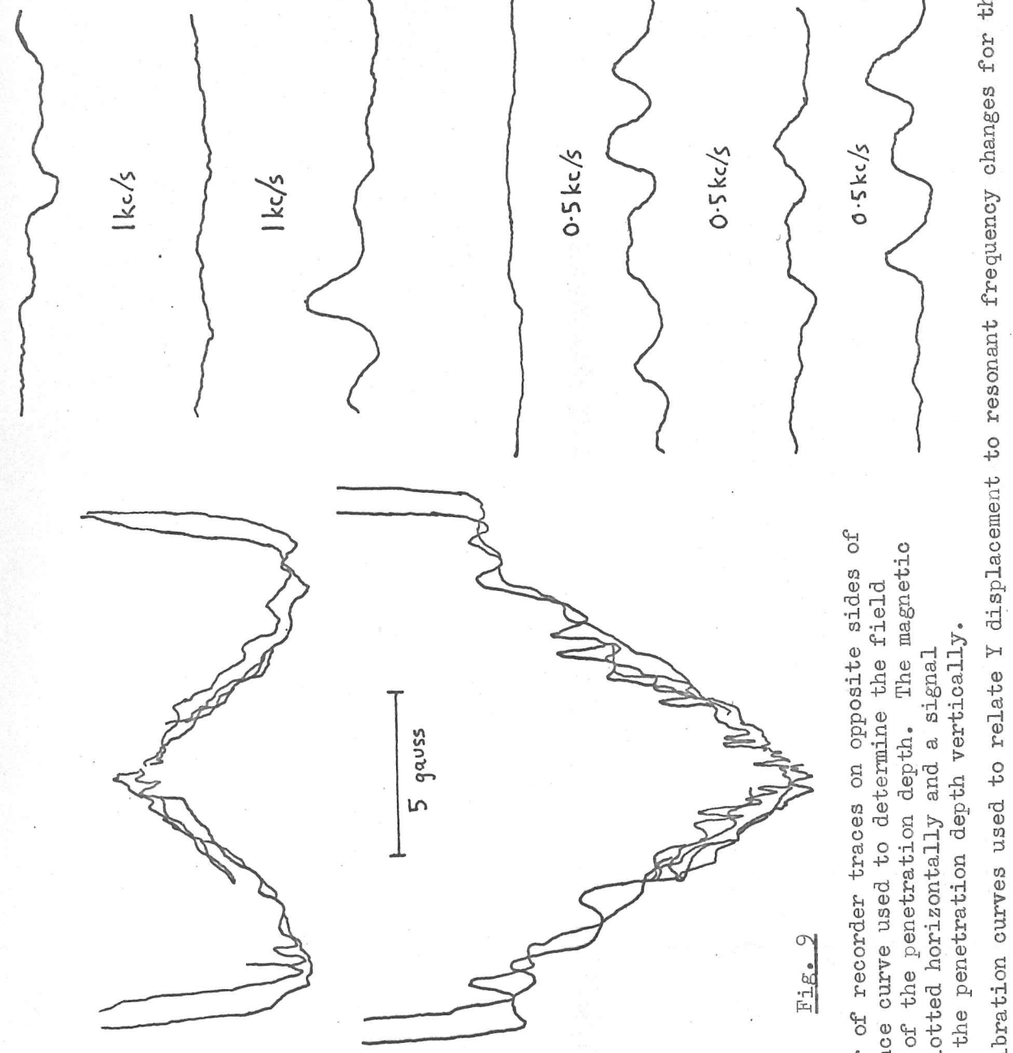

Fig. 9

Left: pair of recorder traces on opposite sides of the resonance curve used to determine the field dependence of the penetration depth. The magnetic field is plotted horizontally and a signal related to the penetration depth vertically.

Right: calibration curves used to relate Y displacement to resonant frequency changes for the traces on the left.

field. A typical X-Y reconder plot, including traces giving the relation between output and oscillator frequency, is shown in fig. 9.

(vii) Miscellaneous observations and calibrations

Critical field curve

The critical field of the specimen was measured at various temperatures by setting the oscillator so that the specimen was in the centre of the resonance, and measuring output as a function of applied longitudinal field, the coupling to the loop being made fairly strong. When the specimen became normal the Q of the resonance dropped, causing the output to increase. There was a tendency for supercooling to occur, and for the transition to occur in a series of steps, but there was a fairly well defined maximum transition $\frac{\text{field}}{\Lambda}$ in increasing fields, and this was taken as defining the critical field.

Critical temperature and transition width

The critical temperature of the specimen was obtained from the critical field curve as the temperature where the critical field extrapolated to zero. To find the width of the transition, the range of fields over which the transition took place at constant temperature was estimated from the curves used to find the critical fields close to the critical temperature, and this range was then converted to a value of the broadening of the critical temperature in zero field, using the slope of the critical field curve near the transition point.

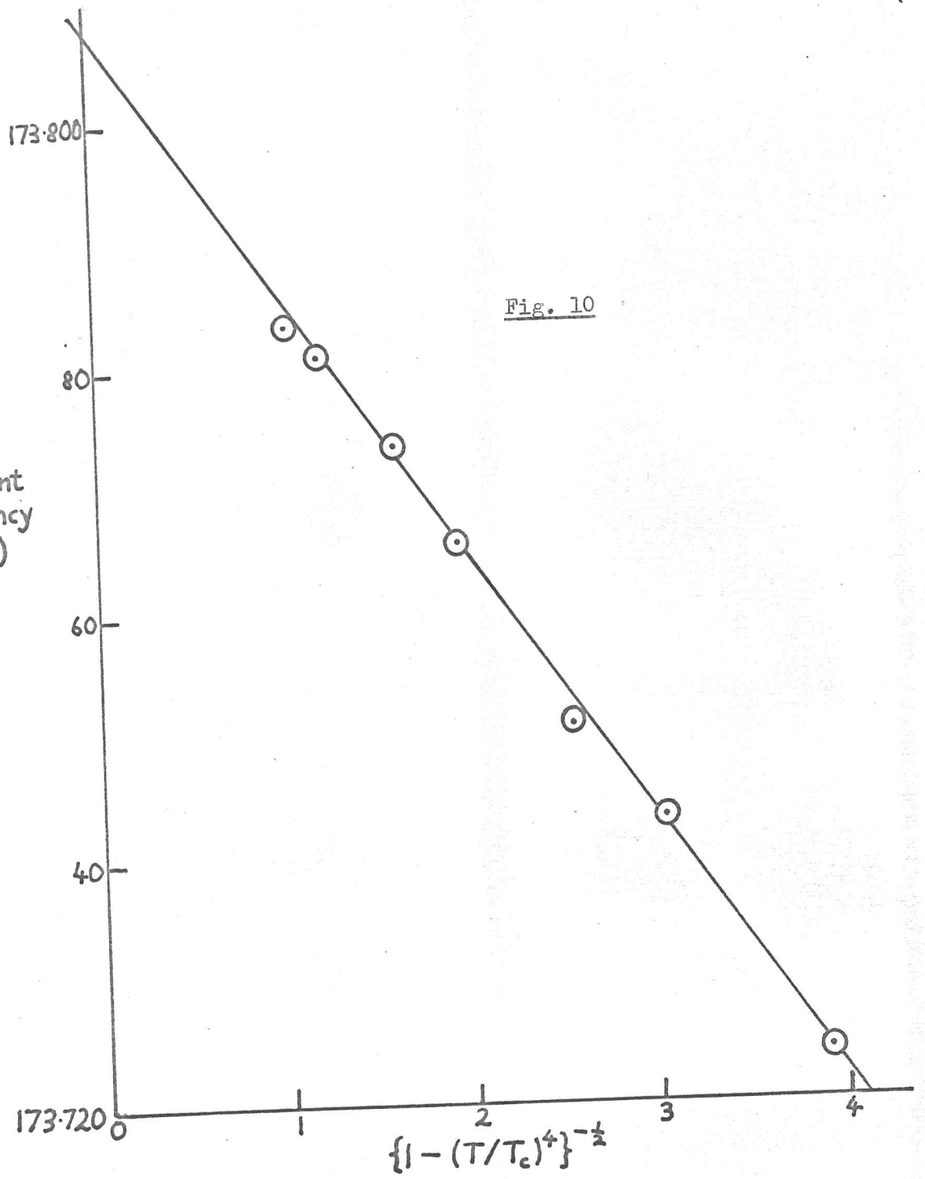

Fig. 10

Constants relating magnetic fields and currents through the magnets

The fields corresponding to a given current in the magnets were found by comparison with a standard solenoid made by Dr. Faber. A search coil connected to a ballistic galvanometer was used to compare the magnetic fields.

Constant relating resonant frequency changes to changes in penetration depth

The resonant frequency changes observed in the experiment are proportional to the changes in penetration depth, the constant of proportionality depending on the detailed geometry of the system. In the past, methods of varying degrees of sophistication have been used to determine this constant, but here we have adopted a fairly simple approach, as follows. Resonance curves were plotted in zero field at different temperatures (a typical plot is shown in fig. 8). At such low frequencies as those used in the present experiment the penetration depth in zero field is proportional to $z \equiv (1-(T/T_c)^4)^{-\frac{1}{2}}$ over a fairly wide range of temperatures. This is confirmed by the experimental plot of resonant frequency against z (fig 10). By extrapolating the linear portion of the curve to z=0 the frequency corresponding to zero penetration depth was found. The experimental curve was then used to find the frequency change corresponding to the penetration depth at any temperature. The method described was used to present all the experimental results as fractional changes in penetration depth at the temperature concerned.

Residual resistivity ratio

The residual resistivity ratio of the specimen was measured by

breaking the capillary at the ends of the specimen and soldering leads to it. The specimen was connected in series with a standard resistor and the voltages appearing across each were compared at room temperature and liquid helium temperature by means of a potentiometer, the currents being reversed to allow for thermal e.m.f's.

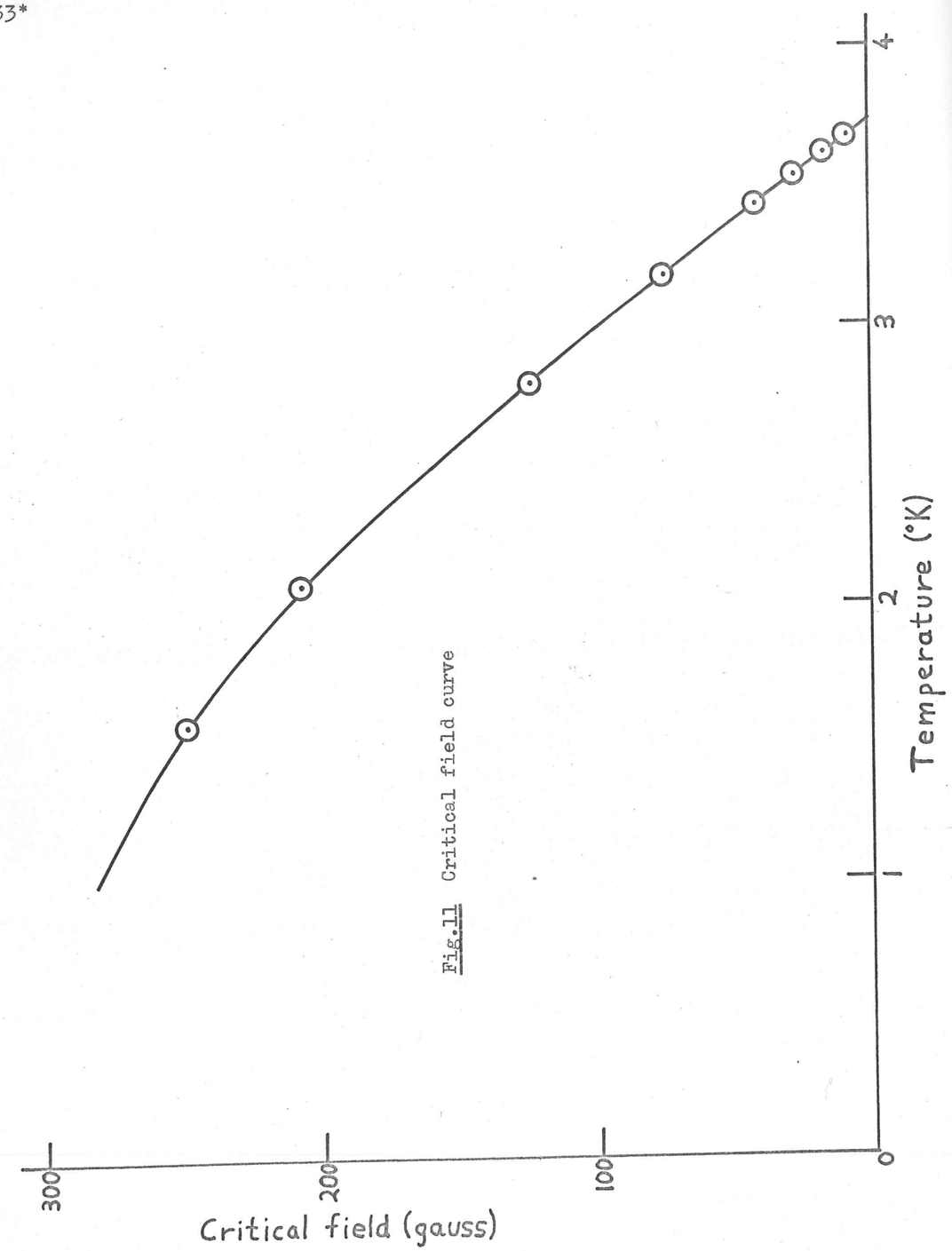

Fig.11 Critical field curve

Chapter 3. Results and discussion

(i) Specimen characteristics

The characteristics of the specimen are given in the following table.

TABLE I. Specimen characteristics

Material	Johnson Matthey 'spec. pure' tin
Total length	105 cm.
Room temperature resistance (291°K)	9.10 ohms
Residual resistance (4.2°K)	1.232 milliohms
Residual resistivity ratio	7390
Mean diameter	0.0144 cm.
Relaxation time (4.2°K)	1.55×10^{-10} sec.
Mean free path (4.2°K)	0.0084 cm.
Transition temperature	3.715°K
Transition width (field)	2.2 gauss
Transition width (temperature)	0.015°K = 0.004 T_c
Critical field curve	see fig. 11
Resonant frequency	174 Mc/s

The determination of most of the quantities in table I has been described already. The mean diameter was determined from the room temperature resistance, assuming a resistivity of 1.4×10^{-5} ohm cm. (from the Chemical Rubber Publishing Company Handbook of Chemistry and Physics 1962-3). The relaxation time and mean free path at helium temperature were obtained from the observed resistivity and data for tin given by Fawcett (1960).

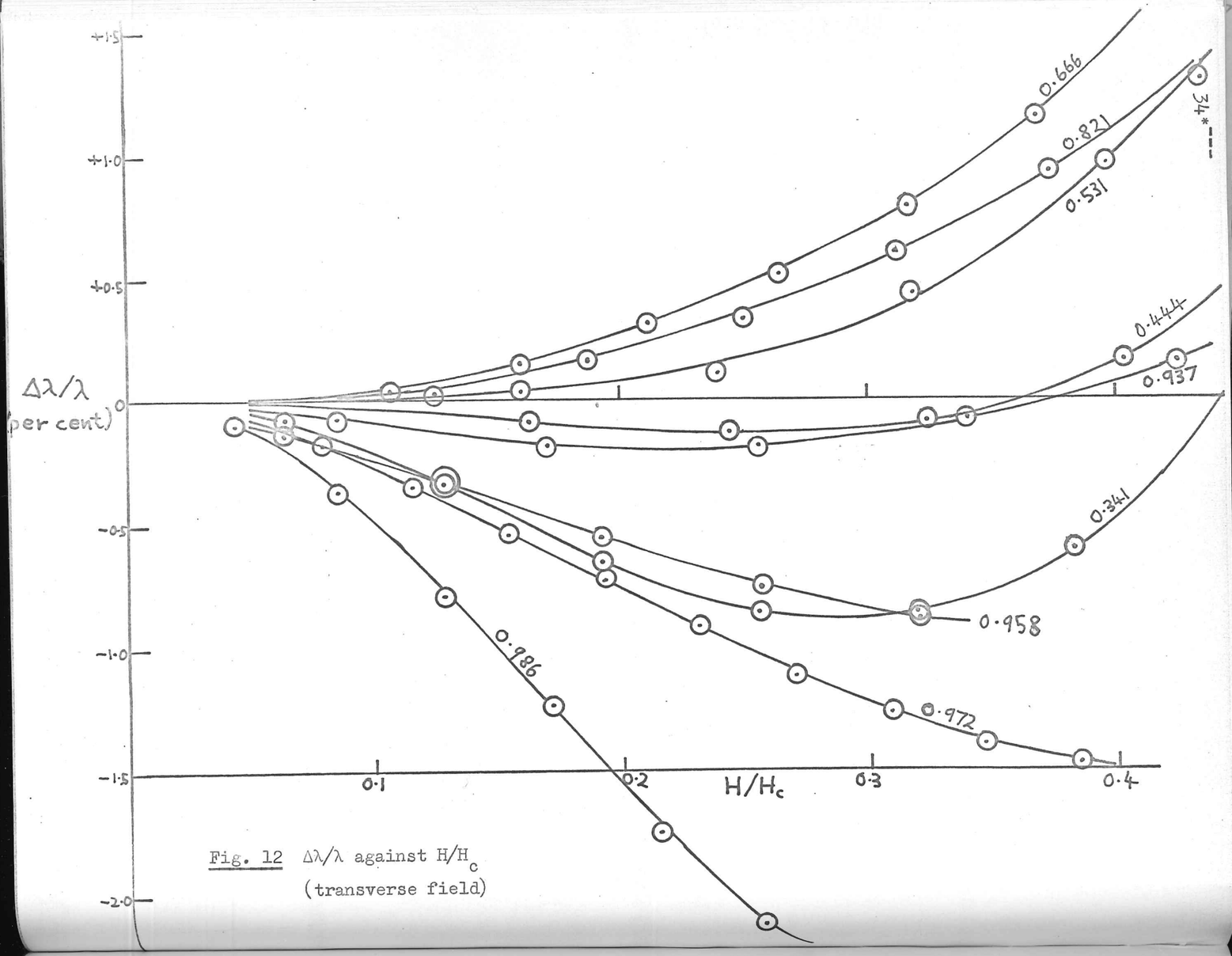

Fig. 12 $\Delta\lambda/\lambda$ against H/H_c
(transverse field)

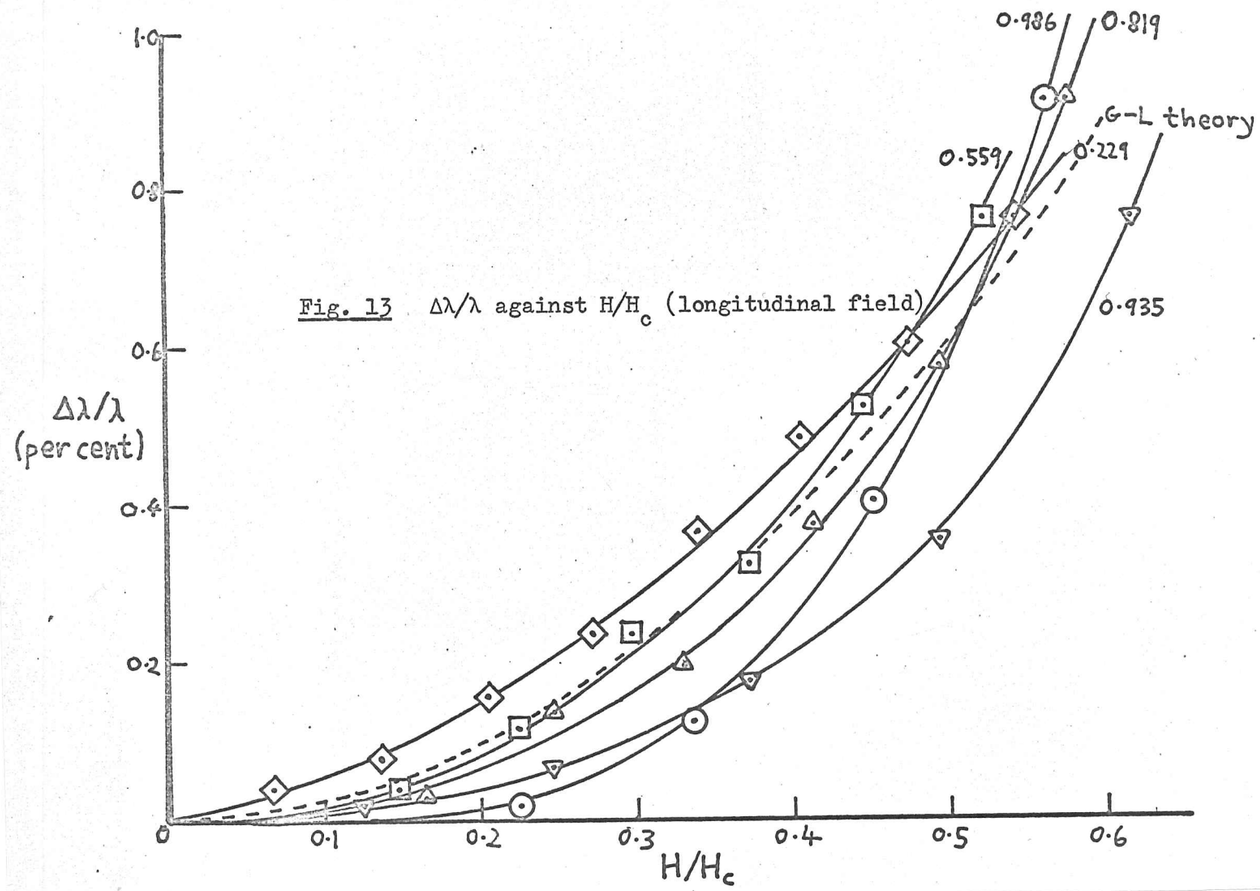

Fig. 13 Δλ/λ against H/H_c (longitudinal field)

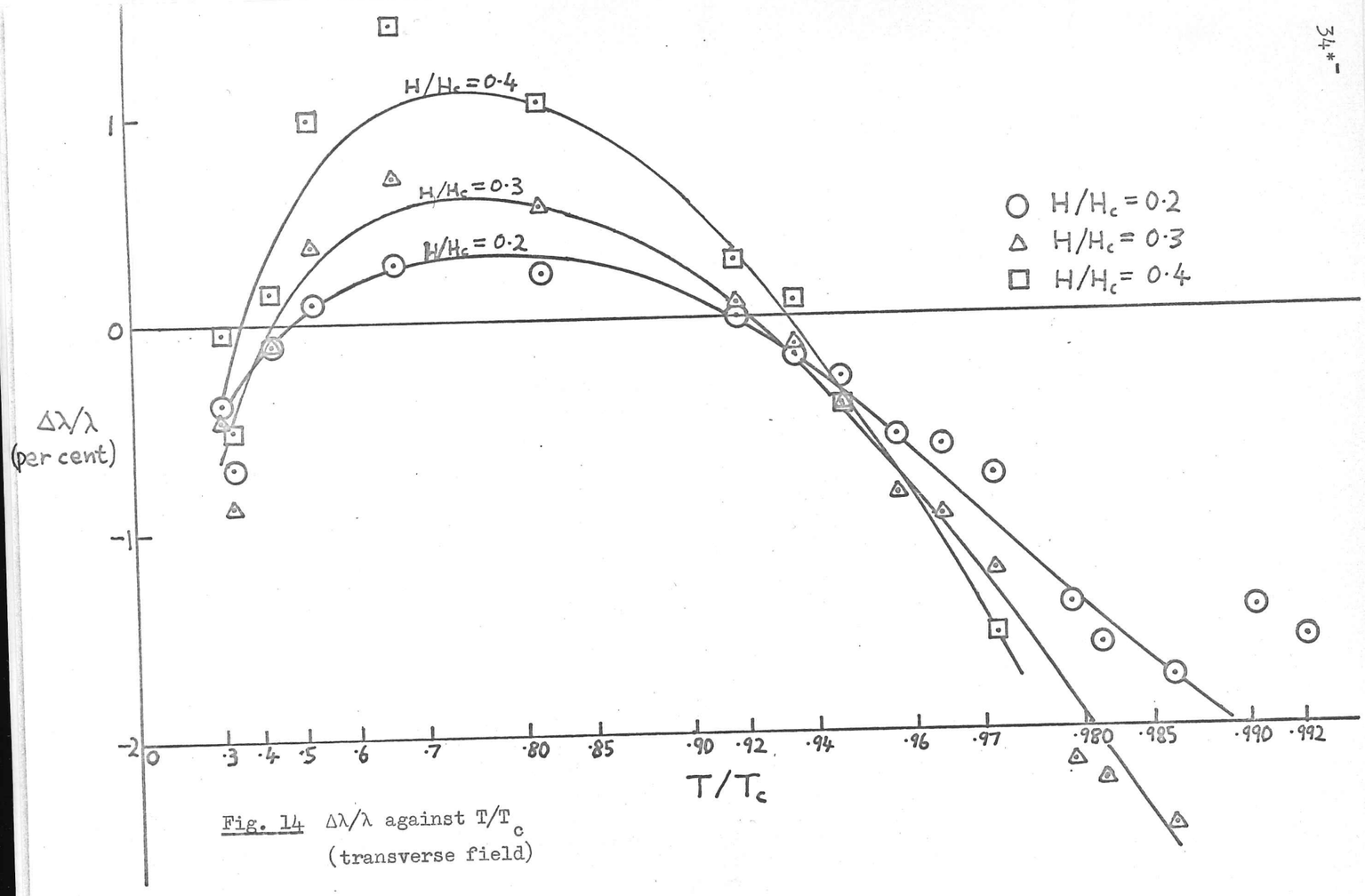

Fig. 14 $\Delta\lambda/\lambda$ against T/T_c
(transverse field)

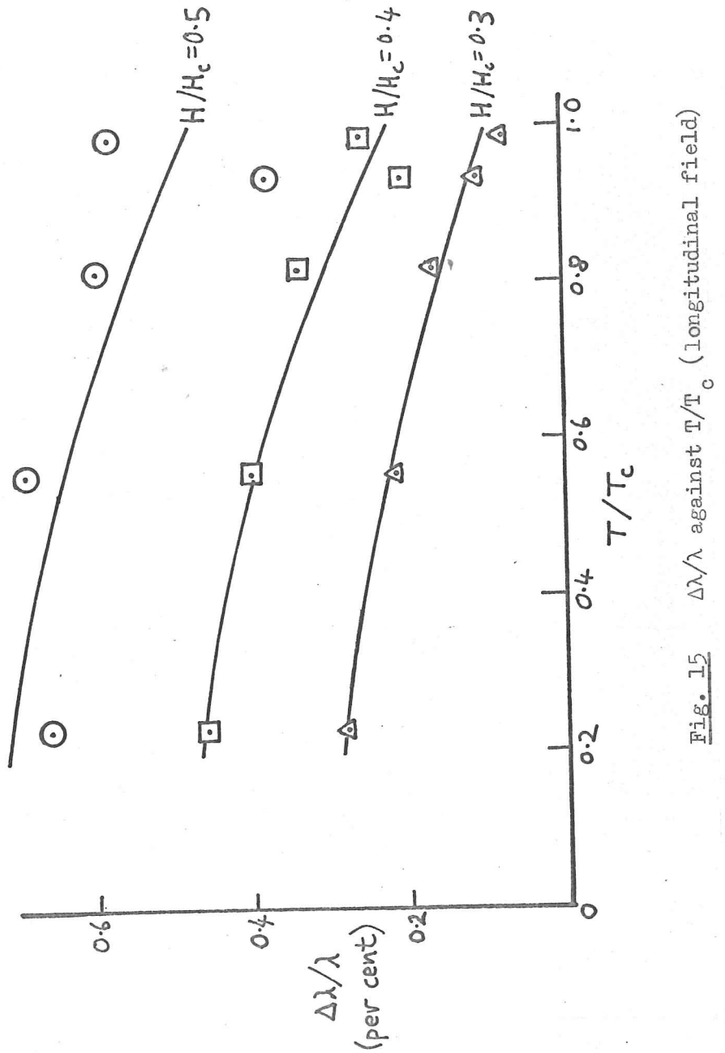

Fig. 15 $\Delta\lambda/\lambda$ against T/T_c (longitudinal field)

The crystal orientation of the specimen was not measured, but owing to its shape it is unlikely that solidification would have proceeded gradually from one end to the other, and so the specimen probably consisted of a large number of differently oriented crystals of length of the order of 1 cm.

(ii) The field dependence of the penetration depth

The experimental results are tabulated in tables II and III (next page). The magnetic fields are given in gauss and the frequency changes $\Delta\nu$ in kc/s. The results are displayed graphically in figs. 12-15. In figs 12 and 13 the fractional penetration depth change $\Delta\lambda/\lambda_{\text{reduced}}$ is plotted against the reduced magnetic field $h = H/H_c$ for various temperatures in the transverse and longitudinal cases, and in figs. 14 and 15 $\Delta\lambda/\lambda$ is plotted as a function of reduced temperature for various values of h, using interpolated values of $\Delta\lambda/\lambda$ obtained from the curves of figs. 12 and 13. For clarity some curves have been omitted from fig. 12, but fig 14 contains the points derived from the omitted curves as well. In fig. 14 temperature has been plotted on a logarithmic scale to expand the region near T_c.

(iii) Errors

Almost certainly the main source of error in the experiment was that caused by the irregular mechanical disturbances to the specimen mentioned in chapter 2, section vi. The pen recorder trace reproduced in fig. 9 was taken at a temperature where the change in

(continued on page 37)

EXPERIMENTAL DATA ON THE FIELD DEPENDENCE OF THE PENETRATION DEPTH

Note In tables II and III the left hand column is the temperature in degrees Kelvin. The pairs of numbers to the right are the experimental observations, the upper member of the pair being the field in gauss and the lower member the observed resonant frequency change in kc/s.

Table II Transverse field

3.686	0.14	0.28	0.43	0.57	0.71	0.85				
	0.18	0.44	0.86	1.27	1.70	2.00				
3.679	0.14	0.28	0.43	0.57	0.71	0.85	0.99	1.14		
	0.06	0.26	0.70	1.02	1.32	1.64	1.88	2.06		
3.664	0.28	0.57	0.85	1.14	1.42	1.70	1.99			
	0.09	0.34	0.74	1.15	1.63	1.97	2.28			
3.647	0.57	1.14	1.70	2.27	2.84					
	0.24	0.65	1.07	1.48	1.79					
3.637	0.57	1.14	1.70	2.27	2.84	3.41				
	0.12	0.46	0.88	1.15	1.50	1.72				
3.610	0.57	1.14	1.70	2.27	2.84	3.41	3.98	4.54	5.11	5.68
	0.04	0.14	0.27	0.42	0.56	0.71	0.86	0.98	1.08	1.14
3.584	0.71	1.42	2.13	2.84	3.55	4.26	4.97	5.68		
	0.04	0.10	0.18	0.27	0.35	0.42	0.50	0.57		
3.558	1.4	2.8	4.3	5.7	7.1					
	0.07	0.18	0.30	0.41	0.48					
3.520	1.4	2.8	4.3	5.7	7.1	8.5	9.9	11.4		
	0.03	0.09	0.13	0.15	0.18	0.21	0.22	0.21		
3.479	2.8	5.7	8.5	11.4	14.2	17.0				
	0.03	0.08	0.08	0.03	-0.07	-0.23				
3.414	2.8	5.7	8.5	11.4	14.2	17.0	19.9			
	0.00	0.00	0.00	-0.01	-0.05	-0.11	-0.20			
3.050	5.7	11.4	17.0	22.7	28.4	34.1	39.8	45.4		
	0.00	-0.01	-0.05	-0.10	-0.18	-0.27	-0.38	-0.53		

Table II (continued)

2.47	8.5	17.0	25.6	34.1	42.6	51.1	59.6	68.2	76.7
	0.00	-0.01	-0.04	-0.08	-0.13	-0.20	-0.29	-0.42	-0.64
1,97	17	34	51	68	85	102			
	0.00	-0.01	-0.03	-0.11	-0.24	-0.51			
1.65	17	34	51	68	85	102			
	0.00	+0.02	+0.03	+0.02	-0.04	-0.21			
1.26	17	34	51	68	85	102	119		
	+0.03	+0.08	+0.16	+0.21	+0.21	+0.15	-0.02		
1.19	17	34	51	68	85	102	119		
	+0.02	+0.05	+0.09	+0.12	+0.11	+0.06	-0.08		

Table III Longitudinal field

3.662	0.85	1.69	2.54	3.38	4.23			
	0.00	-0.02	-0.11	-0.35	-0.79			
3.473	4.2	8.4	12.7	16.9	21.1			
	-0.01	-0.03	-0.08	-0.16	-0.34			
3.041	7.6	15.2	22.8	30.4	38.0	45.6	53.2	
	0.00	-0.01	-0.04	-0.06	-0.11	-0.17	-0.27	
2.076	15	30	46	61	76	91	106	
	0.00	-0.01	-0.03	-0.06	-0.08	-0.13	-0.19	
1.0	19	38	57	76	95	114	133	152
	-0.01	-0.02	-0.04	-0.06	-0.09	-0.12	-0.15	-0.19

penetration depth was large, and most traces had considerably worse signal to noise ratio than fig. 9. The values of $\Delta\nu$ given in Table I were derived not from the recorder traces themselves but from hand-drawn smooth curves drawn on top of the traces following the general trend of the traces but with the noise removed. Traces where the noise was so great that the location of such a curve was doubtful were discarded. The procedure described is somewhat subjective, but in view of the non-random nature of the noise probably gave better results than an exact integration procedure would have done. However, since the points of the curves of figs. 12 and 13 have themselves been derived via hand-drawn curves, no information can be deduced from the accuracy with which they lie on the curves drawn. This comment is not applicable to figs. 14 and 15, since there the points on a given curve correspond to different temperatures and involve independent calculations from a set of different recorder traces. Therefore an estimate of the random errors can be obtained from the scatter of the points in figs. 14 and 15. This indicates that the absolute error in $\Delta\lambda/\lambda$ should be generally less than 0.2% in the transverse case and 0.1% in the longitudinal case, the corresponding relative errors being of the order of 15%.

The errors in temperature determination above 1.5°K, where the pressure was determined from the mercury manometer, would be important only near T_c. Any systematic errors would affect the determination of T_c in the same way, and hence not affect T/T_c, while random errors

are small compared with the width of the transition in zero field. Temperature determinations below 1.5°K using the McLeod gauge are liable to be too great by an amount of the order of 0.1°K, owing to the presence of a leak which was not noticed at the time in the connection to the McLeod gauge.

The broadening of the transition ($\Delta T_c/T_c = 0.004$) should not be important except for the two highest temperatures at which observations were carried out. These observations appear only in fig. 14, and it can be seen that the points for the temperatures concerned do indeed deviate appreciably from the curve.

The earth's magnetic field is approximately a quarter of that corresponding to the width of the transition, and should therefore not have had an important effect on the results. The errors in field determination and the inhomogeneities of the field over the specimen were both small compared with the errors in the determination of $\Delta\lambda$.

Various other possible sources of error were investigated. A trace was taken in the usual way with the specimen off resonance, using somewhat greater magnetic fields and sensitivities than those used during the penetration depth measurements, and it was found that the magnetic field had no detectable effect on the amplitude of the output of the oscillator. It also had no significant effect on its frequency.

Another possible source of error would occur if the magnetic

field could exert a mechanical force on the superconducting specimen and displace it relative to the screening can, thus altering the resonant frequency. To investigate this possibility, the Helmholtz coils were moved from their symmetrical position so as to create a strongly inhomogeneous field near the specimen, and the effect on the recorder trace noted. There was no appreciable effect apart from a small change in the scale of the X axis due to the change in the field at the specimen, indicating that magnetic forces on the specimen were not a significant source of error.

Another source of error which must be considered is that at the ends of the zig-zag the current is flowing in a different direction to that elsewhere, causing a mixing of the longitudinal and transverse field configurations. One observed effect of this was that the Q of the resonance decreased sharply at fields of the order of $\frac{1}{2}H_c$ in both the longitudinal and transverse field configurations. However, from the short length of the end sections one would estimate that the error introduced by them in fields smaller than those required to produce the sharp decrease in Q would be less than five per cent, except possibly in the longitudinal case near T_c, where an appreciable reduction in the observed value of $\Delta\lambda/\lambda$ might result.

Finally, there is the question of whether the surface of the specimen was suitable for this type of experiment. Not very much can be said on this point, but as will be seen later the observations in the longitudinal field case are in fair quantitative agreement with the predictions of the G-L theory, which increases confidence

in the validity of the observations in the transverse case (where agreement with the G-L theory is not expected). Sharvin and Gantmakher (1961) found that straining their specimens considerably increased the value of α (eqn. 6, chapter 1), but this may not be a relevant point here as they were using a considerably different frequency.

In summary, it would appear that the results obtained should show the correct general behaviour of the penetration depth in a magnetic field, but that the vibratory disturbances to the specimen have prevented results more accurate than about 15% from being obtained.

(iv) Discussion of the results

Longitudinal field

It will be seen from fig. 15 that the value of $\Delta\lambda/\lambda$ for given longitudinal h is not strongly temperature dependent, changing by only a factor of 2 over the temperature range covered. The effect tends to become less as the transition temperature is approached. Assuming a value for κ of 0.16, the prediction of the G-L theory has been plotted in fig.13, and it is seen that it is in fair agreement with the experimental results. These conclusions are in agreement with those found at 2 Mc/s for their good specimens by Sharvin and Gantmakher (1961). However, it should be pointed out that the region of validity of the G-L theory for tin is quite small (i.e. $T/T_c \gtrsim 1-\kappa^2$. See, for example Gor'kov 1960), so that agreement would be expected only for the curve $T/T_c = 0.986$ in any

case. The region where the G-L theory is not valid has, it is believed, not been investigated theoretically.

Transverse field

In the transverse field case there is no resemblance at all between the predictions of the G-L theory and the experimental results. For example, for h=0.4, the G-L theory predicts a $\Delta\lambda/\lambda$ of 2.3% (allowing for the averaging effect discussed in the appendix, which increases $\Delta\lambda/\lambda$ by a factor 2), while the maximum observed at any temperature is 1.1%. More significantly, the maximum value of the ratio in the transverse and longitudinal cases is only 0.6 times that expected in the quasi-static limit (6, allowing for the averaging effect). Furthermore, for temperatures above about 0.93 T_c and below about 0.45 T_c $\Delta\lambda/\lambda$ even has the wrong sign. These observations are in disagreement with those at 2 Mc/s, where the G-L theory gives good agreement with experiment as in the longitudinal case, but are more similar to those obtained at higher frequencies (1 and 3 Gc/s). However, at the higher frequencies the low temperature sign reversal of $\Delta\lambda/\lambda$ does not occur and the high temperature sign reversal occurs at a lower temperature (of the order of 0.75 T_c as opposed to 0.93 T_c). These differences could possibly be due to anisotropy effects.

One observation which may be important in testing any theory which may be proposed to explain the experiments is the detailed shape of the $\Delta\lambda/\lambda$ against H curves (figs. 12 and 13). In the longitudinal case these are roughly parabolic (as predicted by the G-L

theory), as also in the transverse case in the region defined approximately by $0.5\ T_c < T < 0.85\ T_c$. At low temperatures in the transverse case there is an H^4 term in $\Delta\lambda/\lambda$ sufficient to cause its sign to change from negative to positive as H is increased. More interesting, however, is the behaviour near T_c. At temperatures near $0.97\ T_c$ the behaviour is quite well approximated by the law $\Delta\lambda/\lambda \propto |H|$. This relation implies that the quadratic approximation, $\lambda(H) = \lambda(0)\{1 + \alpha(H/H_c)^2\}$, which must be a good one in the limit $H \to 0$, must break down in very small fields. Indeed, the breakdown occurs at such a low field that it is best seen not in the plotted curves but in the original recorder traces. Fig. 9, taken at $0.972\ T_c$, is a good example. Owing to the noise on the recorder traces it is difficult to tell exactly where the quadratic approximation breaks down, but the following observations can be made:

(i) As T is reduced the range of h over which the quadratic approximation is valid becomes less, the corresponding field H being roughly constant and of the order of 0.5 gauss.

(ii) At the temperature where the effect is most pronounced ($\sim 0.97\ T_c$) the quadratic approximation is valid only over a range $|h| < 0.1$ or less.

(iii) The effect is visible in traces taken down to $0.937\ T_c$, but at lower temperatures becomes lost in the noise.

The effect observed cannot be explained as due to the earth's magnetic field, whose only effect would be to tend to smear out such an effect if it existed. A similar remark would apply to explanations

based on inhomogeneities of the specimen or the field, and it does not appear possible either to explain the effect as due to the presence of normal regions. It is, of course, possible that smearing out of the effect has occurred in the present case, and that the field concerned is even smaller than 0.5 gauss.

The same effect has also been observed at higher frequencies, though not so clearly, since observations were not made in very small fields, as they were in the present experiment. In particular, the curves plotted by Spiewak (1958) at 3.320°K and by Richards (1962) at 0.894 T_c are similar to the curve of fig. 9.

It would clearly be desirable for the effect in small fields to be investigated further, using compensating coils for the earth's field and a detection system which measured $\frac{d\lambda}{dH}$ or $\frac{d^2\lambda}{dH^2}$ directly.

(v) Summary of the discussion of results

(i) In a longitudinal field $\Delta\lambda/\lambda$ is always positive and is roughly in accordance with the G-L theory.

(ii) In a transverse field $\Delta\lambda/\lambda$ is negative at low temperatures and near T_c, and positive otherwise. The observations bear no relation to the predictions of the G-L theory, but are in many ways similar to those at higher frequencies.

(iii) There is evidence that in the transverse case near T_c the quadratic approximation for the dependence of λ on H breaks down in very small fields, of the order of 0.5 gauss.

Appendix The unconvolution of the integrals occurring in the transverse field configuration

When a transverse field H is applied to a cylindrical superconducting wire the field at a point on its surface is $2H\sin\phi$, where ϕ is the angle between the field direction and the radius vector to the point. This local field h (we abandon previous notation for this appendix) is position-dependent and in general different from H, so that when one measures a field-dependent quantity such as the penetration depth, which in a local field h has a value f(h), what one obtains is not f(H) (H=applied field) but an average over the surface of the cylinder

$$\bar{f}(H) = \frac{2}{\pi}\int_0^{\pi/2} f(2H \sin\phi)\, d\phi \qquad (1)$$

where it is assumed that f depends on the magnitude of h only and not on its direction.

It is easily verified that if f(h) has the form $a+bh^2$ then $\bar{f}(H)$ is $a+2bH^2$, a fact we have used previously in this chapter. In general, however, f will be a more complicated function and the question arises how f can be found if $\bar{f}$ is known (the unconvolution problem), and whether the solution is unique. This problem has not in general been attempted in the past, in the belief that its solution would involve a tedious trial and error procedure. The object of this appendix is to show that such a procedure is not necessary. A simple analytic solution will be derived and applied to an experimental curve.

Consider the expression

$$I(H) \equiv \int_0^H f(\eta)\,d\eta$$

$$= H\int_0^{\frac{\pi}{2}} f(H\cos\theta)\sin\theta\,d\theta \quad (\text{putting } \eta = H\cos\theta)$$

$$= \frac{2H}{\pi}\int_0^{\frac{\pi}{2}} d\phi \int_0^{\frac{\pi}{2}} f(H\cos\theta)\sin\theta\,d\theta$$

$$= \frac{2H}{\pi}\int_{\phi=0}^{\pi/2}\int_{\theta=0}^{\pi/2} \sin\theta\,d\theta\,d\phi\,.f(H\cos\theta)$$

$$= \frac{2H}{\pi}\iint f(H\cos\theta)\,dS$$

where the last integral is over an octant of a unit sphere and θ, ϕ are polar coordinates.*

Going over now to Cartesian coordinates

$$x = r\sin\theta\cos\phi$$
$$y = r\sin\theta\sin\phi$$
$$z = r\cos\theta$$

we obtain

$$I = \frac{2H}{\pi}\iint_{\substack{\text{unit}\\ \text{sphere}\\ x>0,\ y>0,\ z>0}} f(Hz)\,dS$$

whence by symmetry we deduce

$$I = \frac{2H}{\pi}\iint_{\substack{\text{unit}\\ \text{sphere}\\ x>0,\ y>0,\ z>0}} f(Hy)\,dS$$

$$= \frac{2H}{\pi}\int_{\phi=0}^{\pi/2}\int_{\theta=0}^{\pi/2} \sin\theta\,d\theta\,d\phi\,f(H\sin\theta\sin\phi)$$

$$= \frac{2H}{\pi}\int_0^{\pi/2}\sin\theta\,d\theta\int_0^{\pi/2} f(H\sin\theta\sin\phi)\,d\phi$$

---

* Writing as an ex-mathematican to physicists, I suppose it is necessary here for me to interject the remark that the sphere has no physical significance whatever. This appendix may serve as a good example of the fact that out of mathematical abstraction may come results which are useful to the physicist (as it is hoped fig. 16 will demonstrate).

Figure 16

(i) Experimental curve
(ii) Calculated unconvoluted curve
(iii) Curve obtained from (ii) by averaging

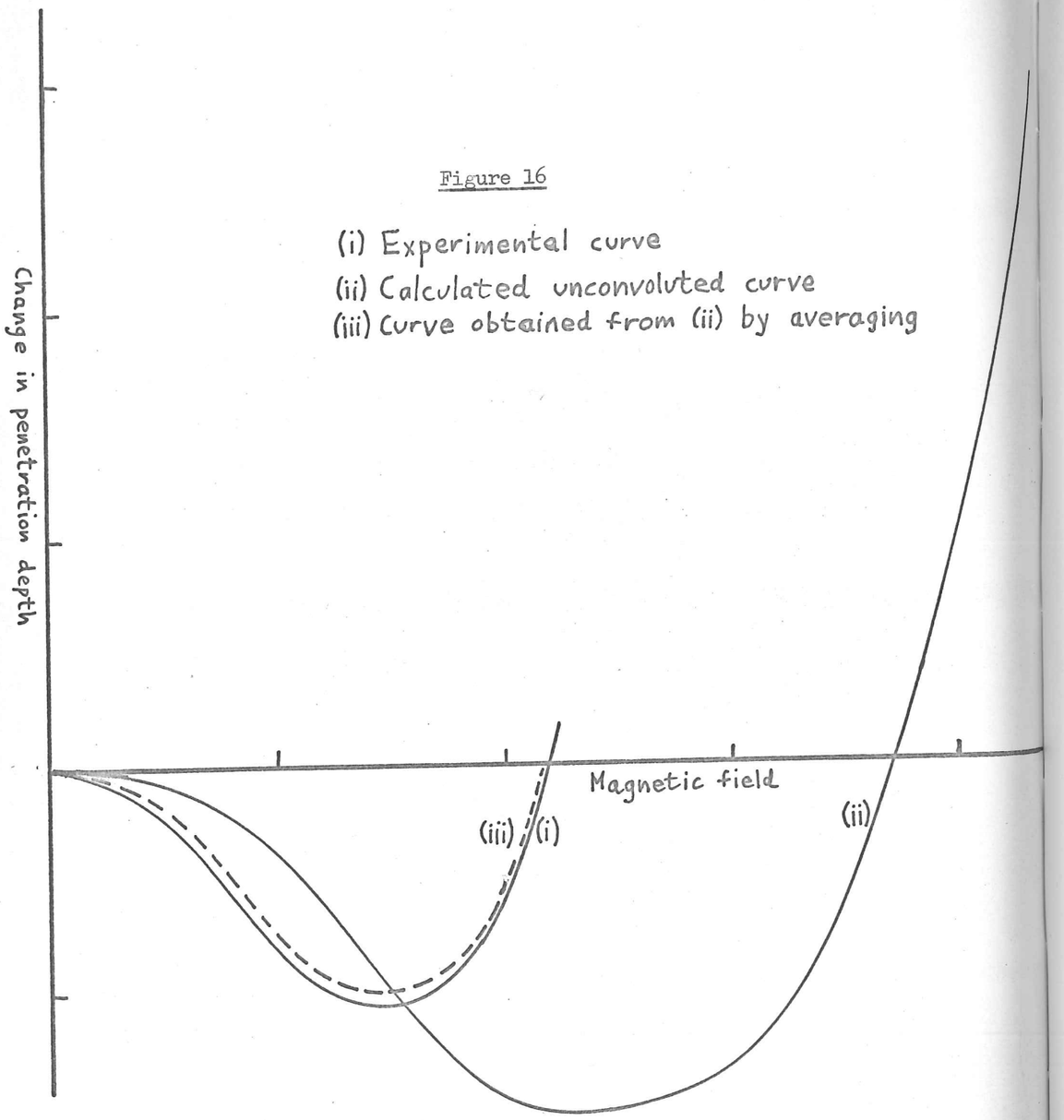

$$= H \int_0^{\pi/2} \bar{f}(\tfrac{1}{2}H \sin\theta) \sin\theta \, d\theta \quad \text{from (1)}$$

Combining this result with the definition of I(H), we obtain

$$f(H) = \frac{dI}{dH}$$

$$= \frac{d}{dH}\left\{ H \int_0^{\pi/2} \bar{f}(\tfrac{1}{2}H \sin\theta) \sin\theta \, d\theta \right\} \qquad (2)$$

which provides an explicit solution to the unconvolution problem. If $\bar{f}$ is known for fields up to H_o, equation (2) gives f uniquely for fields up to $2H_o$. In particular, although one can carry out measurements in a transverse field only up to about $\frac{1}{2}H_c$, information can be obtained about the local behaviour in all fields up to H_c.

Equation 2 was tried out on the values of $\overline{\Delta\lambda/\lambda}$ from the observations in a transverse field at 0.341 T_c (curve (i) of fig. 16). Curve (ii) is the $\Delta\lambda/\lambda$ curve obtained by substituting in eqn. (2). Finally, the values of $\Delta\lambda/\lambda$ obtained were substituted back in eqn. (1), giving curve (iii). It will be observed that the agreement between (i) and (iii) is quite good, considering the rather crude methods which were used to perform the integrations.

I am indebted to Mr. N. Th. Varopoulos for drawing my attention to the fact that a problem to which the present one can be transformed was solved by the mathematician Abel in the nineteenth century. Abel's work appears not to have been used previously in connection with the present problem.

In view of the fact that the unconvolution process in this and other cases investigated produced no important changes in the general shape of the curves, it was decided that it was not worth doing a systematic unconvolution of all the results. In any case, any

theoretical formula can be convoluted to compare with the experimental results more quickly than the experimental results can be unconvoluted to compare with the theory, as the former operation need be done only once to deal with all the results.

Chapter 4 Theory

In this chapter the theories which have been put forward to attempt to explain the anomalous (negative) sign of $\Delta\lambda/\lambda$ will be described.

Firstly there is the theory of Dresselhaus and Dresselhaus (1960). This theory assumes a simple two-fluid model, with the superfluid obeying the Londons'equation and the normal fluid being described by the Boltzmann equation, allowing for the effect of the magnetic field in bending the orbits of the normal electrons. Some features of the observations can be explained qualitatively, but the theory has the following defects:

(i) A detailed fit of the theory to the observations requires the effective mass of the normal electrons to be less by a factor of nearly 10^3 in some cases than it is in the normal state (Richards 1962).

(ii) The theory does not account for the fact that the large deviations from the G-L theory are confined to the transverse case.

(iii) The theory does not account for the small-field breakdown of the quadratic approximation for λ.

(iv) The anomalous effects at low temperatures observed in the present experiment cannot be explained on the theory since at such low temperatures the number of normal electrons is negligible.

(v) The theory does not explain the observations of Richards on the effects of impurities (Richards 1962).

We turn next to the theory of Bardeen (1958). Bardeen assumed that a wave disturbance analogous to that of second sound in superfluid helium might be possible in superconductors. In such a

wave the oscillating quantity would be not the total density of electrons as in plasma oscillations but instead the temperature and the order parameter n_s. Since in the surface impedance experiments a transverse magnetic field but not a longitudinal one causes oscillations in n_s (chapter 1), second sound can be excited in the former case but not the latter. By some mechanism not specified in detail by Bardeen, this might cause the anomalous sign of $\Delta\lambda/\lambda$ in the transverse case. In addition the effects might be larger near T_c owing to the larger number of normal electrons present there, while the effect of adding impurities might be to damp out the second sound waves, thus explaining the observations of Richards.

Although some type of collective excitation similar to second sound may be responsible for the effects observed, it does not seem likely that the type occurring in helium can occur under the conditions of the experiments. In second sound in helium the normal fluid undergoes 'hydrodynamic flow'. By this is meant that there is local equilibrium, with non-zero mean velocity, of the excitations of the normal fluid, caused by excitation-excitation collisions, which do not alter the total momentum of the normal fluid. Under the conditions of the experiments on surface impedance, the electron-electron collision relaxation time is long compared with the relaxation time for the decay of a normal current through collisions of the normal electrons with the boundaries of the specimen or with impurities. Hence hydrodynamic flow of the normal electrons is not possible. Furthermore, in the Bardeen theory, the

wavelength of the second sound is supposed to be of the order of the penetration depth. This is considerably shorter than the mean free path in the experiments on pure tin, so that again the conditions for treating the motion of the normal electrons as hydrodynamic flow are violated.

The question arises as to whether a different type of second sound can exist, in which the extreme opposite condition, mean free path $\gg$ wavelength is satisfied. This type of second sound would bear the same relation to the other kind as that of zero sound to ordinary sound in fluids. The possibility has been investigated independently by Thouless (1960) and by Josephson (unpublished), who arrived by different methods at essentially the same dispersion relation. This is very complicated and has not so far been analysed in detail. However, the following conclusions can be stated:

(i) The velocity of such a disturbance if it existed would be of the order of the Fermi velocity, i.e. of the order of 10^4 times as great as that of Bardeen's type of second sound.

(ii) The dispersion equation has no phonon-like solutions at any temperature, with the possible exception of a region close to T_c (a published statement to the contrary by Thouless and Tilley has since been withdrawn following the discovery of a numerical error).

The situation close to T_c has not hitherto been investigated.

It can be seen from the above that so far there is no satisfactory theory to account for all the observations and their complicated dependence on all the parameters involved. Possibly some combination

of the ideas of the Bardeen and Dresselhaus theories may solve the problem, but it seems likely that a new idea may be necessary before a full explanation is obtained.

Part II

SUPERCURRENTS THROUGH BARRIERS

(i) Introduction

The characteristic features of superconducting systems, the Meissner effect, zero resistivity, quantized persistent currents in macroscopic rings and quantized flux lines, are the consequences of a long-range ordering process of an essentially quantum nature. Part II of this dissertation deals with the properties of superconducting systems partitioned by thin barriers of substances which in bulk are not superconducting. Such systems have become the subject of much recent experimental work, in connection with both dielectric barriers (tunnelling) and barriers of normal metals (proximity effects). We shall deal with such questions as the following: What effect does a barrier have on the superconducting long-range order? What happens to the characteristic features of a superconductor as the barrier is made thicker? Are new types of behaviour possible?

What distinguishes superconducting systems from all other systems is a special property of the parameter which describes the ordering process. In normal systems the order parameter (e.g. spin density in a ferromagnetic system) can be uniquely defined irrespective of the gauge chosen for the electromagnetic potentials. This is not so for the order parameter ψ of a superconductor, which changes under a gauge transformation in the same way as do wave functions in elementary quantum mechanics:

$$A \rightarrow A + \text{grad}\ \chi$$
$$\phi \rightarrow \phi - \frac{1}{c}\frac{\partial \chi}{\partial t} \qquad (1)$$
$$\psi \rightarrow \psi \exp\{(ie^*/\hbar c)\chi\}$$

where ϕ and A are the scalar and vector electromagnetic potentials respectively, χ is the scalar function of position defining the gauge transformation and e* is a constant having the dimensions of electric charge. Since there exists a particular gauge transformation (with χ independent of position and time) which multiplies ψ by a constant phase factor and leaves the electromagnetic potentials unchanged, it follows that the phase of ψ is not a physically meaningful quantity; it is only the phase differences between its values at different points of space that are important. The theory of Ginzburg and Landau (1950) assumed an order parameter of this type. It can be shown that the theory leads to a Meissner effect, and to quantized persistent currents and flux lines (Ginzburg and Landau (1950), Abrikosov (1957), Keller and Zumino (1961)). It was shown by Gor'kov (1959) that the existence of an order parameter with the properties postulated follows from the microscopic theory of superconductivity, with e* equal to 2e, the charge of the Cooper pairs present in the superconducting state. It will not be necessary in setting up the phenomenological theory of barriers to consider the exact meaning of the order parameter, and so we shall not deal with this question here.

After these preliminaries let us return to consideration of the properties of barriers. We have seen that the ordering process

consists of a long-range correlation of the phase of ψ. If now a barrier divides a superconductor into two parts, it is clear that if it is thick enough it will prevent the phase correlations getting across it. It should therefore be possible in that case to vary the phases of ψ in the two parts independently of each other. Consider now the opposite extreme of a very thin barrier, which we can think of as being a two-dimensional array of impurity atoms. As its thickness tends to zero we approach a situation in which there is no barrier at all. In the absence of a barrier ψ must vary continuously with position; it is not possible to draw a plane dividing the superconductor into two parts and to alter the phases of ψ in the two parts independently, as this would introduce a discontinuity in ψ in crossing the plane.

We see that as the barrier is changed from a very thick one to a vanishingly thin one the system loses the degree of freedom corresponding to the ability to alter the phases independently as just described. By what mechanism can this loss take place? The answer is the following very simple one. The free energy of the system contains a contribution from the barrier region which depends on the relative phases of the values of ψ on the two sides of the barrier, and whose magnitude becomes greater as the barrier is made thinner. With very thick barriers the free energy contribution from the barrier is negligible and the phases are able to vary arbitrarily with respect to each other. As the barrier is made thinner, however, the barrier energy begins to exert an influence

and the phases become effectively locked together.

A change in behaviour as a function of barrier thickness which is more directly related to experiment is the question of whether a barrier can pass supercurrents, i.e. currents at zero applied voltage. In the limit of a vanishingly thin barrier supercurrents must be able to flow just as in the bulk metal, while thick barriers do not transmit supercurrents. In practice it is observed that tunnelling specimens of resistance less than about an ohm almost invariably show critical supercurrents of the order of milliamps, while specimens of resistance greater than about 10 ohms show no detectable currents at zero voltage. Before discussing the relationship between this observation and the phase locking, it will be convenient to consider the relationship between long-range order and zero resistivity in superconductors in general.

Let us consider in the first place a normal metal in a state not too far removed from equilibrium (e.g. a wire fed from a current generator). It is then possible to define approximately a local chemical potential for electrons (the Fermi level). Quasi-particles continuously move about from one part of the metal to another, tending to produce an equilibrium state with the same chemical potential everywhere. However, since the quasi-particles move only a short distance between collisions, it is quite possible to have a situation where there is local equilibrium everywhere without general equilibrium, i,e. the chemical potential can change slowly with position. Furthermore, it is only in non-equilibrium

states that non-zero currents can occur, since only then is there anything to determine in which direction the currents should flow. This situation can be avoided in the case of the superconductor, as we shall see, by assuming that the time dependence of the order parameter is related to the local chemical potential. The exact form of the relation can be obtained by extending a basic result of the Gor'kov (1958) theory, according to which the order parameter of a superconductor in equilibrium at a chemical potential μ is everywhere proportional to $e^{-2i\mu t/\hbar}$. The natural extension of this result to non-equilibrium situations is that the rate of change of the phase of the order parameter at any point is equal to $-\frac{2}{\hbar}$ times the local chemical potential. This assumption is consistent with the gauge transformation (1). From it one can deduce that in a steady state there can be no potential differences in a superconductor if long range phase correlations are present in ψ, since a difference in the potential at two points would result in the phase relationship between the values of ψ at the two points changing with time.

The possibility of deriving zero resistance from long range order in this way is confined to superfluid systems, since only in these does the order parameter transform under gauge transformations in such a way as to allow a suitable expression for the chemical potential to be obtained. It should be noted also that the existence of a position-dependent order parameter permits currents to occur even when the chemical potential is independent of position, since their magnitude and direction can be determined by the details of the spatial variation of the order parameter.

Returning now to the effects of phase locking in barriers, by a similar argument we see that if there is phase locking zero voltage supercurrents of magnitude determined by the phase relationships between the values of ψ on the two sides of the barrier may occur, but if the phases are not locked then the usual mechanism for maintaining the potential of the superconductor the same everywhere is absent, and only resistive currents can flow across the barrier.

(ii) Basic phenomenological formulae

In this section we shall derive a set of phenomenological formulae with which to investigate the macroscopic properties of barriers. While in the derivation of these formulae from microscopic theory it may well be necessary to consider the full details of how quantities such as ψ vary as one goes through the barrier, it is clear that as far as macroscopic phenomena are concerned the problem is essentially a two-dimensional one, and we must first consider what set of physical quantities is necessary to specify the problem. In the first place let us consider the following set:

(i) the order parameters on each side of the barrier.

(ii) the currents and magnetic fields in the neighbourhood of the barrier.

(iii) the potential difference across the barrier.

A difficulty arises in connection with the quantities (ii), since owing to the smallness of the penetration depth these quantities

should be regarded as varying in three dimensions. To avoid excessive complications we shall here deal only with situations where the regions on each side of the barrier extend away from the barrier for distances large compared with the penetration depth, and that magnetic fields if they are present are appreciable only in the neighbourhood of the barrier. In this case we can assume that the magnetic fields are parallel to the barrier and are determined uniquely, according to some penetration law, by the field in the barrier itself. This device reduces the problem back to two-dimensional form, since only the field in the barrier need appear in the equations. Generalization to the case of thin films separated by a barrier could be obtained by including also the fields at the outside edges of the films, but we shall not attempt this here.

For our purposes the set of quantities (i) is more than we require. We shall be interested here only in small magnetic fields and currents, which do not appreciably affect the magnitude of the order parameter but only its phase. Furthermore, only <u>differences</u> in the phase of the order parameter are physically meaningful. It follows that the effects of the order parameter in the neighbourhood of a point of the barrier can enter only through the difference between the values of its phase on the two sides.

For simplicity we shall assume that the barrier is flat and occupies the plane z=0. The quantities required to specify the problem are now

(i) $\phi(x,y,t) \equiv \arg \psi(x,y,0+,t) - \arg \psi(x,y,0-,t)$, the change in the phase of ψ as one crosses the barrier from negative z to positive z,

(ii) $H_x(x,y,t)$ and $H_y(x,y,t)$, the components of the tangential magnetic field in the barrier,

(iii) $V(x,y,t) \equiv \frac{1}{e}\{\mu(x,y,0-,t) - \mu(x,y,0+,t)\}$, the potential difference across the barrier,

and (iv) $j_z(x,y,t)$, the current through unit area of barrier.

We must now derive equations relating these quantities. Firstly, from Maxwell's equations we have

$$\frac{\partial H_y}{\partial x} - \frac{\partial H_x}{\partial y} = \frac{4\pi j_z}{c} + \frac{1}{c}\frac{\partial D_z}{\partial t} \qquad (2)$$

The displacement current term must be included since there may be large electric fields in the barrier. An expression for it may be found by regarding the barrier as a capacitor. Since the normal component of D in the region between the plates of a capacitor is equal to 4π times the charge per unit area on its plates, the displacement current may be expressed in terms of C, the self-capacitance of the barrier per unit area, and the potential difference V across it, giving the result

$$\frac{\partial H_y}{\partial x} - \frac{\partial H_x}{\partial y} - \frac{4\pi C}{c}\frac{\partial V}{\partial t} = \frac{4\pi j_z}{c} \qquad (3)$$

Next we must find equations giving the time and spatial variations of ϕ. Firstly, from the relation assumed (section (i)) between the chemical potential and the rate of change of the phase of ψ, which may be written as

$$\frac{\partial}{\partial t} \arg \psi = - \frac{2\mu}{\hbar} \qquad (4)$$

we obtain the equation

$$\frac{\partial \phi}{\partial t} = \frac{2e}{\hbar} V \qquad (5)$$

To derive a formula for the spatial variation of ϕ is rather more difficult. The problem was first solved by Anderson (private communication), who pointed out that the situation was similar to those occurring in the phenomena of interference between electron beams in the presence of a magnetic field (Ehrenberg and Siday 1949) and of flux quantization in superconductors. By using gauge invariance he was able to prove the following result (Anderson and Rowell 1963, Anderson 1963): consider two points P and Q on opposite sides of the barrier and outside the region of the magnetic field, joined by two curves crossing the barrier at different points A and B. The difference between the phases of ϕ at A and B is proportional to the flux enclosed between the two curves, one flux quantum hc/2e corresponding to a phase difference of 2π. This result may also be obtained directly from the Ginzburg-Landau equations, by similar calculations to those used by Keller and Zumino (1961) in their treatment of flux quantization. In differential form the result may be written:

$$\frac{\partial \phi}{\partial x} = \frac{2ed}{\hbar c} H_y$$
$$\frac{\partial \phi}{\partial y} = - \frac{2ed}{\hbar c} H_x \qquad (6)$$

where d is the effective thickness of the region of magnetic field

near the barrier, i.e. $\{\int_{-\infty}^{\infty} H(z)dz\} / H(0)$. d is equal to $\lambda_1+\lambda_2+t$, where λ_1, λ_2 are the penetration depths on each side of the barrier and t is the barrier thickness.

One more equation is needed to complete the description of the system, namely an expression for the current through the barrier, j_z. This can only be obtained from basic theory, which we defer to section (vi), but the most important features can be deduced from general considerations. Firstly we recall that in the situation where phase locking occurs there is a zero voltage supercurrent through the barrier which is determined by the phase difference. We may therefore write in this case:

$$j_z = j_z(\phi) \tag{7}$$

j_z must of course be a periodic function owing to the nature of ϕ. In the more general case (V non-zero and ϕ time-dependent) we must expect that extra terms will have to be added to the right-hand side of (7). One such term will be the term corresponding to the ohmic currents across the barrier, which will be a function of V. In the case in which V is constant and the transmission coefficient through the barrier for quasi-particles is assumed to be small compared to unity, j_z is given (Josephson 1962) by an expression of the form

$$j_z = j_1(V) \sin \phi + \{\sigma_0(V) + \sigma_1(V) \cos \phi\}V \tag{8}$$

In deriving the macroscopic properties of barriers we shall keep only the term in (8) corresponding to zero-voltage supercurrents, on the grounds that this term should be the chief factor in determining

the basic properties, though it must be borne in mind that we are thereby leaving out of consideration all damping effects, which are due to the terms omitted. We shall therefore replace (8) by the relation

$$j_z = j_1 \sin \phi \tag{9}$$

with a constant j_1. Equations (3), (5), (6) and (9) are the required set of equations for providing a complete phenomenological description of the behaviour of barriers. From them can be derived an equation involving only ϕ:

$$\nabla^2 \phi - \frac{1}{v^2} \frac{\partial^2 \phi}{\partial t^2} = \lambda^{-2} \sin \phi \tag{10}$$

where

$$v = c/(4\pi dC)^{\frac{1}{2}} \tag{11}$$

$$\lambda = (\hbar c^2/8\pi j_1 ed)^{\frac{1}{2}} \tag{12}$$

and ∇^2 is the two-dimensional operator $\frac{\partial^2}{\partial x^2} + \frac{\partial^2}{\partial y^2}$. Since (10) is a non-linear partial differential equation, it will not be possible to obtain the general solution, and we shall confine ourselves to considering important limiting cases.

(iii) Thermodynamics

In this section we shall derive a relationship between the supercurrent through a barrier under equilibrium conditions and the free energy associated with the barrier. This can be used to investigate the stability of time-independent solutions of the equations derived in the last section. The proof given here is based on a gedankenexperiment, in the spirit of classical thermodynamics. A more mathematical type of proof has been given by

Anderson (1963).

Since we expect both the free energy associated with the barrier and the current density through it to be determined by the local value of $\emptyset$, it will be sufficient in deriving the relationship between them to consider a barrier so small that the spatial variations of $\emptyset$ over it may be neglected. Let us consider two systems A and B, which are identical except for the fact that A contains a barrier and B does not, i.e. B is a single superconducting region. Suppose that A and B are connected to generators supplying an identical current I to each. The free energies of A and B will be functions F_A, F_B respectively of I. If I is changing voltages V_A, V_B will appear across A and B. Equating the free energy changes to the work done by the generators, we obtain

$$dF_i = V_i I dt \quad (i=A \text{ or } B)$$

so that $$d(F_A - F_B) = (V_A - V_B) I\, dt.$$

Now since A and B are identical except for the barrier, $F_A - F_B$ is simply F, the free energy associated with the barrier, and $V_A - V_B$ is equal to V, the voltage across the barrier.

Hence $$dF = VI\, dt = \frac{\hbar}{2e} \frac{\partial \emptyset}{\partial t} I\, dt = \frac{\hbar}{2e} I\, d\emptyset$$

so that $$I = \frac{2e}{\hbar} \frac{dF}{d\emptyset} \qquad (13)$$

Expressing (13) in terms of quantities per unit area, we obtain the more generally valid result

$$j_z = \frac{2e}{\hbar} \frac{\partial f}{\partial \emptyset} \qquad (14)$$

where f is the barrier free energy per unit area. In the special

case of eqn. (9), therefore, we obtain for the barrier free energy per unit area:

$$f = -\frac{\hbar}{2e} j_1 \cos\phi + \text{const.} \qquad (15)$$

(iv) Equilibrium properties

If ϕ is independent of time, (10) reduces to

$$\nabla^2\phi = \lambda^{-2} \sin\phi \qquad (16)$$

This equation was first derived by Anderson (private communication) and by Ferrell and Prange (1963).

If the transverse dimensions of the barrier are small compared with λ, one solution of (16) has ϕ approximately constant. It then follows from (9) that j_z is also constant over the barrier, and takes its maximum value j_1 when ϕ is equal to $\pi/2$. In this case j_1 therefore has the interpretation of the critical supercurrent per unit area of barrier.

Interference of supercurrents

A more general solution of (16), obtained by neglecting the right-hand side, and valid when j_1 and consequently λ^{-2} is small, is

$$\phi = \frac{2ed}{\hbar c}(H_y x - H_x y) + \alpha$$

where H_x, H_y and α are constants. From (6) we see that this is a solution with a constant field $(H_x, H_y, 0)$ in the barrier. This is the solution which will be set up when an external field $(H_x, H_y, 0)$ whose direction lies in the plane of the barrier, is applied to the barrier. The total current through the barrier is then given by

$$I = \int j_1 \sin \phi \, dS = \mathrm{Im} \int j_1 \exp\left\{i\left(\frac{2ed}{\hbar c}(H_y x - H_x y) + \alpha\right)\right\} dS$$

$$= \mathrm{Im}\left[e^{i\alpha} \int j_1 \exp\left\{\frac{2ied}{\hbar c}(H_y x - H_x y)\right\} dS \right]$$

where Im denotes the imaginary part and the integrals are taken over the barrier. The critical supercurrent through the barrier is given by the maximum value of this expression with respect to changes in α, and is

$$I_c = \left| \int j_1 \exp\left\{\frac{2ied}{\hbar c}(H_y x - H_x y)\right\} dS \right| \qquad (17)$$

The integral occurring in (17), regarded as a function of a two dimensional vector (H_x, H_y), is simply the Fourier transform of j_1, with suitable scaling factors and rotated through a right angle. This fact allows us to make the following observation: the square of the critical current through the barrier, regarded as a function of the magnetic field applied to the barrier, is similar in functional form to the Fraunhofer diffraction pattern of an aperture having the same shape as the barrier and transmission coefficient everywhere proportional to j_1. The field dependence of the critical current has been studied experimentally in two cases. For a rectangular barrier (17) predicts a critical current for fields parallel to an edge of the barrier of the form $|(\sin x)/x|$, with minima occurring when the flux enclosed by the barrier is a non-zero multiple of the flux quantum. Behaviour of this type has been observed by Rowell (1963). The second case is the analogue of the interference pattern produced by two coherent point sources, and has been investigated by Jaklevic et. al. (1964), whose experimental

arrangement consisted of two tunnelling barriers connected in parallel. The critical current of the combination was found to be approximately a periodic function of the applied field. It is interesting to note that according to (17), the critical current of the barriers connected in parallel is in general less than the sum of the critical currents which each barrier would have if measured by itself. As pointed out by Jaklevic et. al., their experiment shows that the range of the superconducting long-range order is at least as great as the separation of the two barriers, which in one case was as great as 3.5 mm.

The Meissner effect and the mixed state

Another case of interest occurs when ϕ is everywhere small, so that in (16) sin ϕ can be replaced by ϕ. (16) then reduces to

$$\nabla^2\phi = \lambda^{-2}\phi \qquad (18)$$

This is simply the Londons' equation in two dimensions, and implies that in small magnetic fields there will be a Meissner effect, i.e. currents and magnetic fields will be confined to a region near the edge of the barrier and will fall off with distance from the edge as $e^{-r/\lambda}$. Anderson (private communication) and Ferrell and Prange (1963) have pointed out that this effect will reduce the critical current even in zero magnetic field below the value corresponding to a current density of j_1 per unit area.

For typical barriers used in tunnelling experiments λ is of the order of 1 mm.

Let us now consider qualitatively what will happen in the general

case, given by equation (16). It is clear that the Meissner effect will be destroyed in sufficiently large fields, just as in bulk superconductors, because the exclusion of the magnetic field increases the Gibbs free energy of the system, and in sufficiently large fields this increase cannot be compensated by the lowering of barrier energy obtained by having ϕ everywhere small in the interior of the barrier. The situation when the Meissner effect has been destroyed is analogous to that occurring in the mixed state of type II superconductors, and the transition to the mixed state will occur when it becomes energetically favourable for a single quantized flux line to enter the barrier. As shown by Abrikosov (1957) in the case of type II superconductors, the critical field is simply related to the Helmholtz free energy per unit length of a flux line. This energy is calculated in the appendix, and the corresponding critical field shown to be

$$H_{c1} = (32\hbar j_1/\pi ed)^{\frac{1}{2}} \qquad (19)$$

This is typically of the order of a gauss.

Ferrell and Prange (1963) have investigated the one-dimensional form of equation (16) and in particular have found the maximum field at the edge of the barrier for which a solution with a Meissner effect (field decaying exponentially at large distances from the edge) is possible. This field they find to be $(\pi/2)H_{c1}$, i.e. greater than the thermodynamic transition field. The solutions with $H > H_{c1}$ must be metastable. The explanation for their existence, as in the case of type II superconductors (Bean and Livingston 1964),

is that there is an attractive force between a flux line and the edge of the barrier, so that a flux line has to overcome a potential barrier before it can get into the interior of the barrier. Similarly, metastable solutions corresponding to the mixed state can occur in all applied fields down to zero field.

We have so far assumed the barrier to be homogeneous. Let us now consider briefly the effects of inhomogeneities. As in the case of type II superconductors inhomogeneities will tend to pin the flux lines (Anderson 1962), and this will lead to the possibility of supercurrents being carried by the interior of the barrier as well as by its edge, the Lorentz force on the flux line being balanced by the pinning force. A particular example of this is the supercurrent carried by a superconducting bridge across the barrier.

(v) Non-equilibrium properties

In this section we shall confine ourselves to the case of dielectric barriers, since in the case of normal metal barriers the damping effects due to shunting of the supercurrents by normal currents will be very important and cannot be neglected.

Non-equilibrium properties of barriers can be classified into two types, according to whether there is a dc voltage across the barrier or not. According to (5), in the former case ϕ will increase progressively with time, so that oscillatory effects will occur through oscillations in $\sin\phi$ and hence in j_z, even in the absence of applied oscillating fields. In the latter case ϕ will

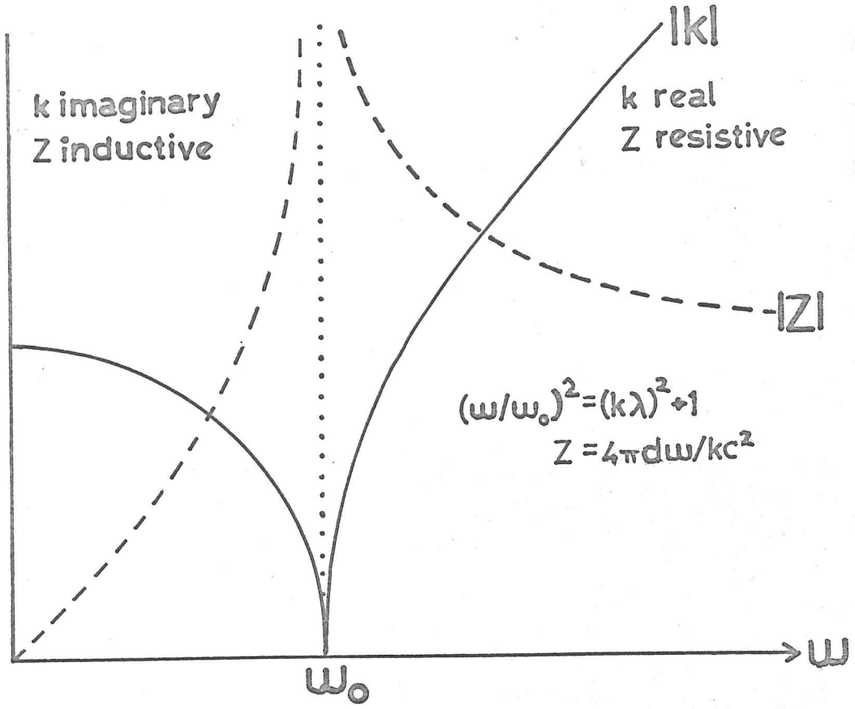

Fig. 17 Frequency dependence of the wave number k and the edge impedance Z for small amplitude electromagnetic waves propagated along a barrier in the absence of steady fields and currents.

oscillate about a mean value, and these oscillations will be damped out by resistive effects unless they are sustained by applied oscillating fields.

The non-equilibrium properties of barriers are described by equation (10):

$$\nabla^2\phi - \frac{1}{v^2}\frac{\partial^2\phi}{\partial t^2} = \lambda^{-2}\sin\phi$$

In the limit of zero supercurrents, i.e. $\lambda^{-2}\to 0$, this reduces to the two-dimensional wave equation. This corresponds to the fact that in this limit the barrier is behaving as a transmission plane (two-dimensional transmission line), the velocity of propagation being v. We shall now consider the properties which depend specifically on the existence of supercurrents.

A. No dc voltage

We shall deal only with the situation in which ϕ undergoes small oscillations about the solution $\phi = 0$, corresponding to zero magnetic field and current, and the barrier is uniform. In this case we may replace sin ϕ by ϕ, obtaining the equation

$$\nabla^2\phi - \frac{1}{v^2}\frac{\partial^2\phi}{\partial t^2} = \lambda^{-2}\phi \qquad (20)$$

On substituting into (20) the plane wave solution $\phi = \exp i(\omega t - k.r)$, we obtain the dispersion relation, illustrated in fig. 17,

$$(\omega/\omega_0)^2 = (k\lambda)^2 + 1 \qquad (21)$$

$$\text{where} \quad \omega_0 = v/\lambda \qquad (22)$$

ω_0 is typically a few Gc/s. It follows from (21) that waves cannot be propagated for $\omega < \omega_0$. In the static limit k tends to i/λ. This

is merely a restatement of the Meissner effect. For $\omega \gg \omega_0$ the propagation velocity tends to v, its value in the absence of supercurrents.

A case of some interest is that for which $\omega = \omega_0$ and $k = 0$. In this case the phase is the same over the whole barrier, and so by (6) there are no magnetic fields. This type of disturbance is in effect a plasma oscillation, reduced in frequency to the microwave region owing to the small density of charge carriers in the barrier, and localized in the barrier owing to its frequency being below the plasma cut-off frequency in the bulk superconductor.

In the $k = 0$ case, in which ϕ is independent of position, we may drop the assumption of ϕ being small, and obtain the pendulum equation (Anderson 1963)

$$\frac{d^2\phi}{dt^2} + \omega_0^2 \sin \phi = 0 \qquad (23)$$

As mentioned previously, in the absence of dc voltages oscillatory disturbances can be set up only if they are excited externally, for example by applying ac voltages across the edge of the barrier. It is therefore of interest to calculate the impedance presented to a source connected across the edge of the barrier, i.e. the voltage across the barrier divided by the current flowing across the edge. The latter is related to the magnetic field in the barrier by Maxwell's equations, so that using equations (5), (6) and assuming for ϕ the plane wave solution, valid in the case of a semi-infinite barrier, we obtain for the edge impedance per unit length

$$Z = 4\pi d\omega/kc^2 \qquad (24)$$

The variation of Z with frequency is shown in fig. 17. Below ω_o Z is purely inductive, while above it Z is purely resistive. This is due to the fact that only above ω_o can travelling waves carry energy away from the barrier.

Owing to the smallness of d, Z is normally very small ($< 10^{-3}$ ohm cm.), but it is larger near ω_o, by an amount depending on the damping of the plasma type oscillation.

The phenomena discussed here could probably be observed in a barrier in the form of a thin-film transmission line, it being necessary of course to ensure that the power applied was not so great as to cause the breakdown of the linear approximation (20).

The separation into normal modes of the type discussed here of the thermal and zero-point fluctuations of $\emptyset$ could be used as the starting point of a calculation of their magnitude, a quantity which would determine whether the phase locking discussed in section (i) would occur. Detailed calculations have hitherto not been performed (see, however, Anderson and Rowell (1963), Anderson (1963) and Josephson (1964) for a qualitative discussion).

B. Finite dc voltage

In this case $\emptyset$ increases progressively with time, so that the approximation that $\emptyset$ is small can no longer be made. In general (10) can only be solved numerically, and the solutions may be expected to have very complicated behaviour, as is confirmed by experimental results (Fiske 1964, Eck et. al. 1964, and various unpublished

observations). For small j_1, however, (10) may be solved approximately by an iterative procedure, thus allowing the main features of the solutions to be seen. To do this we write (10) as two equations:

$$\nabla^2\phi - \frac{1}{v^2}\frac{\partial^2\phi}{\partial t^2} = j_z/(j_1\lambda^2) \qquad (25)$$

$$j_z = j_1 \sin\phi \qquad (26)$$

As a zero order approximation we may solve (25) with the appropriate boundary conditions, putting the right-hand side equal to zero. These boundary conditions will depend on the dc voltage and on what oscillatory fields if any are being applied to the barrier. The value of ϕ obtained can then be substituted into (26) to obtain a value of j_z which is used as the right-hand side of (25) in the next approximation, and so on. We shall now consider separately the cases with an applied oscillating field present or absent.

(a) No oscillating field applied

In this case an appropriate zero order solution of (25) (Eck et.al. 1964) is

$$\phi_0 = \frac{2ed}{\hbar c}(H_y x - H_x y) + \frac{2e}{\hbar} Vt + \alpha \qquad (27)$$

giving

$$j_z = j_1 \sin\left\{\frac{2ed}{\hbar c}(H_y x - H_x y) + \frac{2e}{\hbar} Vt + \alpha\right\} \qquad (28)$$

where V is the dc potential difference and $(H_x, H_y, 0)$ is the steady magnetic field. We see that the supercurrent oscillates with angular frequency $\omega = 2eV/\hbar$ (the ac supercurrent), and that if the magnetic field is non-zero the current distribution varies as in a travelling wave, with velocity $Vc/|H|d$. The value (28) of j_z must now be substituted into (25) to give a first order correction term ϕ_1 to ϕ.

ϕ_1 will oscillate with the frequency ω of the driving term j_z. We shall not here attempt any detailed calculations, but only note two qualitative features. Firstly, ϕ_1 may be expected to be large when ω is near a resonant frequency of the barrier, i.e. a frequency at which the homogeneous equation

$$\nabla^2\phi + \frac{\omega^2}{v^2}\phi = 0 \qquad (29)$$

has a non-zero solution satisfying appropriate boundary conditions. Secondly, ϕ_1 may also be expected to be large when the ratio between the potential difference and the magnetic field is such that the velocity $Vc/|H|d$ of the supercurrent distribution is equal to v, the velocity of propagation of electromagnetic waves in the barrier.

The existence of the ϕ_1 term will show itself experimentally as a modification of the dc current-voltage characteristics of the barrier. However, the equations set up in section (ii) are not sufficient in themselves to treat these modifications. This is because of our neglect of dissipative processes. If a barrier has a dc potential across it and a dc current through it, energy is being continuously supplied to the barrier, and a steady state situation can occur only if there is some mechanism present for dissipating the energy. We may turn this argument round and obtain a qualitative picture of the behaviour of the dc characteristics by noting that any dissipative process must lead to a dc current through the barrier in order that energy can be conserved. The rate of dissipation will be greater when large oscillating electromagnetic fields are present, i.e. when ϕ_1 is large for either

of the reasons considered previously (the $\emptyset_0$ term gives rise only to dc fields when substituted into (5) and (6)). In both these cases the condition for $\emptyset_1$ to be large is one which involves the voltage across the barrier, so that the current-voltage characteristics should show a resonant peak at a particular voltage or voltages. This has been confirmed by detailed calculations in one particular case by Eck et. al. (1964), and from these calculations it can be seen that the excess dc current arises from a distortion of the waveform of the ac supercurrent (cf. also sub-section (b)).

Experimental evidence for the occurrence of both types of resonant process has been obtained. Fiske (1964) has observed step-like characteristics with rapid rises of current at voltages which are independent of magnetic field, though other features of the characteristics are strongly field-dependent just as is the value of the critical zero-voltage supercurrent. The excess currents observed by Fiske are probably due to the excitation of standing waves in the barrier at characteristic resonant frequencies given by (29). The negative resistance portions of the resonant peaks were presumably unstable under the conditions of the experiment and were not observed.

Eck, Scalapino and Taylor (1964) have obtained evidence for the occurrence of the other type of resonant process. They observed characteristics with a resonant peak at a field-dependent voltage given, to within experimental error, by the velocity matching condition $Vc/(|H|d) = v$.

One further case of interest is that of zero magnetic field and

a uniform barrier, which reduces as in the zero-voltage case to the pendulum equation (23). It is clear that in this case there can be no resonant type of behaviour (remember that we are now dealing with solutions in which ϕ increases progressively with time). This conclusion depends specifically on our assumptions of zero magnetic field and barrier uniformity, which allow equation (10) to be reduced to an ordinary differential equation. Some experimental support for it is provided by the observation that when barriers are made by a method which gives good uniformity of barrier thickness the step-like structure often becomes more pronounced in a magnetic field.

For completeness it should be noted that a more complicated type of behaviour is also possible (Shapiro 1963), in which the barrier voltage jumps back and fore between two different values at a rate determined by the external circuit parameters. This behaviour may be due to a negative resistance region of the characteristic, as suggested by Shapiro, or to the fact that the load line of the barrier may not intersect its dc characteristic (as happens in the neon-tube time base).

(b) Oscillating fields applied

When both dc voltages and oscillating fields are applied together to a barrier a new possibility arises; the ac supercurrent resulting from the dc voltage may become locked to the oscillations of the applied field. This can happen only if the ratio between the two frequencies is a simple rational number. If locking of

the ac supercurrent to an applied field of fixed frequency occurs then the dc component of the current is free to vary, since the system has available one degree of freedom corresponding to the possibility of altering the phase relationship between the two oscillations (a specific example will be considered later), while on the other hand the dc component of the voltage is fixed by the voltage-frequency relation (5), since the mean value of $d\phi/dt$ is fixed by the frequency of the field to which the ac supercurrent is locked. This situation is analogous to that occurring in the discussion of the dc supercurrent (section (i)), where the voltage was fixed at zero while the current could vary over a finite range. In the present case the dc characteristics will have a number of constant-voltage regions at finite voltages as well as at zero voltage. The voltage of these regions should be exactly constant as far as the present theory goes, being determined only by the frequency of the applied oscillating field, while in the case of Fiske's experiments the voltage is determined by the frequency of a resonance, which must have a finite width. From a more practical viewpoint we may say that a barrier whose phase oscillations are locked to those of an external oscillator of fixed frequency should behave as a perfect voltage stabilizer, i.e. within limits changing the current through it has no effect at all on the voltage. Pippard (private communication) has pointed out that this property might be used for an accurate determination of the constant h/e on which the voltage-frequency relationship depends.

We shall now make a quantitative analysis in the case where spatial variations may be neglected and j_1 is small. Since j_1 is small, we may assume that the supercurrent has no influence on the voltage across the barrier, which is therefore simply the sum of the applied dc and oscillating potentials:

$$V = V_0 + V_1 \cos \omega t \tag{30}$$

From (5) we therefore obtain

$$\phi = (2eV_0/\hbar)t + (2eV_1/\hbar\omega) \sin \omega t + \alpha \tag{31}$$

so that

$$j_z = j_1 \sin\{(2eV_0/\hbar)t + (2eV_1/\hbar\omega) \sin \omega t + \alpha\}$$

$$= j_1 \sum_{n=-\infty}^{\infty} [J_n(2eV_1/\hbar\omega) \sin\{(n\omega + 2eV_0/\hbar)t + \alpha\}] \tag{32}$$

where J_n is the Bessel function of order n. We see that if $2eV_0/\hbar\omega$ is an integer n then j_z will have a non-zero mean value which depends on the constant of integration α:

$$\overline{j_z} = (-1)^n j_1 J_n(2eV_1/\hbar\omega) \sin \alpha = (-1)^n j_1 J_n(nV_1/V_0) \sin \alpha \tag{33}$$

$\overline{j_z}$ can therefore be either in the direction of the applied dc potential or against it, and to conserve energy power must accordingly be supplied to or absorbed from the applied oscillating field. $\overline{j_z}$ can vary between the limits $\pm j_1 J_n(2eV_1/\hbar\omega)$, so that the size of the step at dc voltage $n\hbar\omega/2e$ is equal to $2j_1 J_n(2eV_1/\hbar\omega)$ and therefore varies in an oscillatory manner with the amplitude of the oscillating component of the field, V_1 (cf. the situation in photon assisted single-particle tunnelling (Tien and Gordon 1963)).

The predicted behaviour of the dc characteristics of barriers in a microwave field, including the possibility expected from (33)

of dc currents flowing in the reverse direction to the applied voltage, has been observed by Shapiro (1963) and Shapiro et. al. (1964). However, in real barriers additional contributions to the current not considered here shift the constant-voltage steps so that they are not symmetrical about zero current as predicted by (33).

(vi) Microscopic theory

The tunnelling Hamiltonian method

The basic problem of the microscopic theory is the derivation of the relation between j_z and ϕ. One method, particularly useful for dielectric barriers, is the tunnelling Hamiltonian method of Cohen, Falicov and Phillips (1962). In this method it is assumed that the Hamiltonian of the system can be written in the form

$$H = H_1 + H_2 + H_T \qquad (34)$$

where H_1 and H_2 are the Hamiltonians for the regions on the two sides of the barrier and H_T is a term describing tunnelling across the barrier, assumed to be of the form $\sum T_{lr} a_l^\dagger a_r$, where a_l and a_r are electron annihilation operators for states on opposite sides of the barrier and H_T is the tunnelling matrix element. The tunnelling Hamiltonian approximation is equivalent to the assumption that tunnelling is an instantaneous process during which the effects of interactions may be ignored.

Since the effects of tunnelling are included entirely in the term H_T, it is reasonable when calculating the tunnelling current to regard this term as a perturbation. For calculating the zero-voltage current the simplest method is to calculate the free energy

of the barrier by perturbation theory and use (14) to derive the supercurrent (Anderson 1963). For calculating the current at non-zero voltage one must use time-dependent perturbation theory. At $t = -\infty$ the system is assumed to consist of two independent subsystems each in equilibrium at different potentials with a definite (time-dependent) value of $\emptyset$. The perturbing term H_T is supposed to be switched on adiabatically and the barrier current resulting is calculated. A calculation in which it was assumed that the Hamiltonians H_1 and H_2 could be approximated by those of non-interacting quasi-particles has been given by Josephson (1962). In this calculation there are certain difficulties in the formalism due to the fact that the usual simplification of measuring all energies relative to the Fermi energy cannot be made since the Fermi level is not the same on both sides of the barrier. This difficulty is related to the fact that $\emptyset$ is time dependent. One way of avoiding it, which has the advantage of not being limited to the weak coupling limit in which independent quasi-particles exist, is to express the correlation functions which enter into the formula for the tunnelling current in terms of Green's functions (Ambegaokar and Baratoff 1963). Two terms are found, one which involves the normal single-electron Green's functions (G functions) and is the same as the expression found for quasi-particle tunnelling by Schrieffer et. al. (1963), and one which involves the Gor'kov F functions and is a periodic function of $\emptyset$. This latter term averages out to zero for non-zero potential differences, so that in an experiment measuring the dc

current-voltage characteristics the formula of Schrieffer et. al. gives the correct result in the approximation used by Ambegaokar and Baratoff. The term involving F functions gives rise to the ac and dc supercurrents, and may be regarded as the contribution from the tunnelling of 'Cooper pairs'. The Cooper pair state (Cooper 1956, Gor'kov 1958) is a boson state of charge 2e whose occupation number is macroscopic. Its existence in superconducting systems is implied by the long-range order of the phase of the order parameter. The energy of the Cooper pair state is twice the Fermi energy, and there is a single state only when the order parameter has phase coherence over the whole of the region which is superconducting.* When a finite voltage is applied across a barrier, the time-dependence of $\emptyset$ implies that phase coherence is present only in each of the sub-regions on either side of the barrier, and instead of a single Cooper pair state there is one state for each side of the barrier. These have different energies owing to the potential difference across the barrier, so that the processes involving tunnelling of Cooper pairs across the barrier are virtual processes. These virtual processes constitute the ac supercurrent. Real processes involving the tunnelling of Cooper pairs, in which the existence of a dissipative process, or the possibility of interaction with photons from a microwave field, allows the energy balance to be kept, are also possible, and have

*An instructive analogy can be found in the behaviour of lasers. When a laser oscillates in a single mode, i.e. a single photon state has macroscopic occupation number, the electromagnetic field has phase coherence over the whole volume of the laser. In this analogy the photons and electromagnetic field of the laser correspond to the Cooper pairs and the order parameter of the superconductor.

been discussed from a different viewpoint in section (v) B.

The magnitude of the zero-voltage supercurrent has been calculated by Anderson (1963) at absolute zero and by Ambegaokar and Baratoff (1963) for finite temperatures. An important result of the calculation is that the supercurrent terms are of the same order of magnitude as the quasi-particle currents occurring at voltages of the order of the energy gap.

The Gor'kov method

It is possible to calculate the zero voltage supercurrent in a way that avoids completely the tunnelling Hamiltonian method and describes propagation through the barrier in terms of Green's functions. This method has the advantages that it shows precisely the factors determining the magnitude of the supercurrent, it indicates the relation between supercurrents through barriers and the usual kind of supercurrent, and it is not restricted to dielectric barriers. The method is based on that used by Gor'kov (1959) to derive the Ginzburg-Landau equations from microscopic theory.

We shall use in our proof the statistical Green's functions G and F^+, defined by

$$G(r\tau, r'\tau') = \langle T(\psi(r,\tau)\psi^\dagger(r',\tau')) \rangle \qquad (35)$$

$$F^+(r\tau, r'\tau') = \langle T(\psi^\dagger(r,\tau)\psi^\dagger(r',\tau')) \rangle \qquad (36)$$

where T is the time-ordering operator and for any operator

$$A(\tau) = e^{H\tau} A e^{-H\tau}$$

For simplicity we shall use units in which $\hbar = 1$, Boltzmann's constant=1

and energies are measured from the Fermi level (so that $\mu = 0$). G and F^+ may be expressed in the usual way as Fourier series:

$$G(r\tau,r'\tau') = T\sum_{\omega} e^{-i\omega(\tau-\tau')}\, G_{\omega}(r,r') \tag{37}$$

the sum being taken over the values $\omega=\omega_n \equiv (2n+1)\pi T$ for integral n, T being the temperature and G_ω being given by the relation

$$G_{\omega}(r,r') = \int_0^{1/T} G(r\tau,r'0)e^{i\omega\tau}\, d\tau \tag{38}$$

with similar relations for F^+. Taking as the single-particle Hamiltonian (including self-energies but ignoring interactions)

$$H_r = \frac{1}{2m}\,(i\nabla_r + \frac{e}{c}\,A(r))^2 + V(r) \tag{39}$$

we may write the Gor'kov equations in the form

$$(i\omega-H_r)G_{\omega}(r,r') + \Delta(r)\, F^{+}_{\omega}(r,r') = \delta(r-r') \tag{40}$$

$$(i\omega-H^{*}_{r'})F^{+}_{\omega}(r,r') - \Delta^{*}(r')\, G_{-\omega}(r',r) = 0 \tag{41}$$

H* being the operator obtained from H by the replacement $i\to -i$. $\Delta(r)=gT\sum_{\omega} F_{\omega}(r,r')$ is the energy gap parameter, g being the interaction constant.

Using the Green's function for non-interacting particles $\tilde{G}_{\omega}(r,r')$, which satisfies the equations

$$(i\omega-H_r)\tilde{G}_{\omega}(r,r') = \delta(r-r') \tag{42}$$

$$(i\omega-H^{*}_{r'})\tilde{G}_{\omega}(r,r') = \delta(r-r') \tag{43}$$

(40) and (41) can be converted into the integral equations

$$G_{\omega}(r,r') = \tilde{G}_{\omega}(r,r') - \int \tilde{G}_{\omega}(r,s)\,\Delta(s)F^{+}_{\omega}(s,r')\, ds \tag{44}$$

$$F^{+}_{\omega}(r,r') = \int \tilde{G}_{\omega}(s,r')\,\Delta^{*}(s)G_{-\omega}(s,r)\, ds \tag{45}$$

Equation (45) is slightly different from Gor'kov's equation, being obtained from it by interchanging G and $\tilde{G}$. This form will be more convenient for our purposes. Obtaining a different equation was the result of using an equation for F^+ derived from the equation of motion for $\psi^\dagger(r')$ rather than the one for $\psi^\dagger(r)$.

F^+ may now be eliminated from (44) and (45), giving the result

$$G_\omega(r,r') = \tilde{G}_\omega(r,r') - \iint \tilde{G}_\omega(r,s)\Delta(s)\, G_{-\omega}(s',s)\Delta^*(s')\tilde{G}_\omega(s',r')\, ds\, ds' \tag{46}$$

The expectation value of the current density,

$$j(r) = \left\langle \left\{ \frac{ie}{m}(\nabla_{r'} - \nabla_r)_{r'=r} - \frac{2e^2}{mc}A(r) \right\} \psi^\dagger(r',0)\psi(r,0) \right\rangle \tag{47}$$

may now be found by expressing it in terms of G (equation 35), as follows:

$$j(r) = -\left\{ \frac{ie}{m}(\nabla_{r'} - \nabla_r)_{r'=r} - \frac{2e^2}{mc}A(r) \right\} G(r,0;\, r',0+) \tag{48}$$

Note that in (47) and (48) is included a factor 2 due to summation over spins. If in the right-hand side of (48) we replace G by $\tilde{G}$, we obtain the current density for a non-interacting system, which is zero in equilibrium. Hence (48) remains true if in it we replace G by $G-\tilde{G}$, and using (37) and (46) we obtain

$$j(r) = T\sum_\omega \left\{ \frac{ie}{m}(\nabla_{r'} - \nabla_r)_{r'=r} - \frac{2e^2}{mc}A(r) \right\} \iint \tilde{G}_\omega(r,s)\Delta(s)\, G_{-\omega}(s',s)\Delta^*(s')\tilde{G}_\omega(s',r')\, ds\, ds' \tag{49}$$

$$= \iint K(r,s,s')\,\Delta(s)\Delta^*(s')\, ds\, ds' \tag{50}$$

where $K(r,s,s') = T\sum_\omega G_{-\omega}(s',s)$

$$\times \left[\frac{ie}{m} \left\{ \tilde{G}_\omega(r,s)\nabla_r \tilde{G}_\omega(s',r) - \tilde{G}_\omega(s',r)\nabla_r \tilde{G}_\omega(r,s) \right\} - \frac{2e^2}{mc}A(r)\tilde{G}_\omega(r,s)\tilde{G}_\omega(s',r) \right] \tag{51}$$

(49) is valid at all temperatures and assumes only the validity of the Gor'kov equations. As a first approximation, valid near T_c where Δ is small, we may replace G by $\tilde{G}$. K then becomes independent of Δ and (49) reduces to Gor'kov's result. Gor'kov derived the Ginzburg-Landau equations from it by assuming Δ to be slowly varying with position and expanding Δ in a Taylor series about the point r. If we are calculating the current at a point in a barrier this approximation is clearly not a good one. However, since K has a range of the order of a coherence length and the important variations in Δ take place over a much smaller range, i.e. the barrier thickness, we may make a different approximation, namely that in the neighbourhood of r Δ takes different constant values Δ_1 and Δ_2 on the two sides of the barrier. (50) then reduces simply to the form

$$j(r) = \sum_{i,j} K_{ij} \Delta_i^* \Delta_j \quad (i,j = 1,2) \qquad (52)$$

Further, no supercurrent can flow across the barrier unless both sides are superconducting, so that the right-hand side of (52) must vanish if either Δ_1 or Δ_2 is zero. Hence $K_{11}=K_{22}=0$. If time-reversal symmetry is present j must change sign when Δ is replaced by Δ^*. In addition j must be real. j therefore reduces to the form

$$j(r) = iK(\Delta_1\Delta_2^* - \Delta_2\Delta_1^*) \qquad (53)$$

where K is real. Putting $\phi = \arg \Delta_2 - \arg \Delta_1$ and $j_1 = \frac{1}{2}K|\Delta_1||\Delta_2|$, this reduces to (9).

More light is thrown on the factors determining the magnitude of the supercurrents if we calculate instead of the current density the

total current through the barrier. Let S be a surface whose intersection with the superconductor lies inside the barrier, and which divides space into two parts V_1 and V_2. If n is a unit vector normal to S pointing into V_2, the total current through the barrier is

$$I = \int\{j(r).n\}\,dS_r = \iint ds\,ds'\,\Delta(s)\Delta^*(s')\int\{K(r,s,s').n\}dS_r \qquad (54)$$

(the suffix r denotes that the surface integral is taken with respect to the point r). The quantity $\int\{K(r,s,s').n\}dS_r$ can be calculated by using the identity

$$\nabla_r\left[\frac{ie}{m}\left\{\tilde{G}_\omega(r,s)\nabla_r\tilde{G}_\omega(s',r) - \tilde{G}_\omega(s',r)\,\nabla_r\tilde{G}_\omega(r,s)\right\} - \frac{2e^2}{mc}A(r)\tilde{G}_\omega(r,s)\tilde{G}_\omega(s',r)\right]$$

$$= 2ie\left\{\tilde{G}_\omega(r,s)\delta(r-s') - \tilde{G}_\omega(s',r)\,\delta(r-s)\right\} \qquad (55)$$

This identity can be proved by direct computation using equations (39), (42) and (43), but it is more instructive to derive it from the law of conservation of charge, as follows. Consider two single-electron states $|s)$ and $|s')$, with wave functions

$$\begin{aligned}\psi_s(r) &= \tilde{G}_\omega(r,s)\\ \psi_{s'}(r) &= \{\tilde{G}_\omega(s',r)\}^*\end{aligned} \qquad (56)$$

respectively. Note that ψ_s and $\psi_{s'}$ are ordinary functions of the position coordinate r and not field operators. From (42) and (43) they satisfy the equations

$$\begin{aligned}H_r\psi_s(r) &= i\omega\psi_s(r) - \delta(r-s)\\ H_r\psi_{s'}(r) &= -i\omega\psi_{s'}(r) - \delta(r-s')\end{aligned} \qquad (57)$$

Now if H_r is a charge-conserving Hamiltonian and $\rho(r)$ is the charge density operator then

$$\nabla_r\, j(r) = -i\left[H_r, \rho(r)\right] \tag{58}$$

so that $\nabla_r \langle s'|j(r)|s\rangle = -i\langle s'|H_r\rho(r) - \rho(r)H_r|s\rangle$

$= \omega\langle s'|\rho(r)|s\rangle + i\langle \delta_{s'}|\rho(r)|s\rangle - \omega\langle s'|\rho(r)|s\rangle - i\langle s'|\rho(r)|s\rangle$

from (57),

$$= i\langle \delta_{s'}|\rho(r)|s\rangle - i\langle s'|\rho(r)|\delta_s\rangle \tag{59}$$

where δ_s, $\delta_{s'}$, are the states with wave functions $\delta(r-s)$, $\delta(r-s')$ respectively. If we now substitute the expressions

$$\langle i|j(r)|k\rangle = -\frac{ie}{2m}\left(\psi_i^*(r)\nabla_r\psi_k(r) - \psi_k(r)\nabla_r\psi_i^*(r)\right) - \frac{e^2}{mc}A(r)\psi_i^*(r)\psi_k(r)$$

$$\langle i|\rho(r)|k\rangle = e\psi_i^*(r)\psi_k(r)$$

and use the definitions (56), then (59) reduces to (55).

and the definition (51)

Using the identity (55), we obtain

$$\int\{K(r,s,s').n\}\,dS_r = \int_{V_1}\nabla_r K(r,s,s')\,dr$$

$$= 2ieT\sum_\omega G_{-\omega}(s',s)\int_{V_1}\left(\tilde{G}_\omega(r,s)\delta(r-s') - \tilde{G}_\omega(s',r)\delta(r-s)\right)dr$$

$$= 2ieT\sum_\omega G_{-\omega}(s',s)\tilde{G}_\omega(s',s)\{n(s') - n(s)\}$$

where n is a function which is equal to 1 in V_1 and 0 in V_2. Noting that the function $n(s') - n(s)$ is zero unless s and s' are on opposite sides of S, we finally obtain

$$I = 2ieT\left(\iint_{s'\in V_1,\, s\in V_2} - \iint_{s\in V_1,\, s'\in V_2}\right) ds\, ds'$$

$$\times\sum_\omega G_{-\omega}(s',s)\,\tilde{G}_\omega(s',s)\,\Delta(s)\,\Delta^*(s') \tag{60}$$

It will be observed that (60) has the desirable property that the

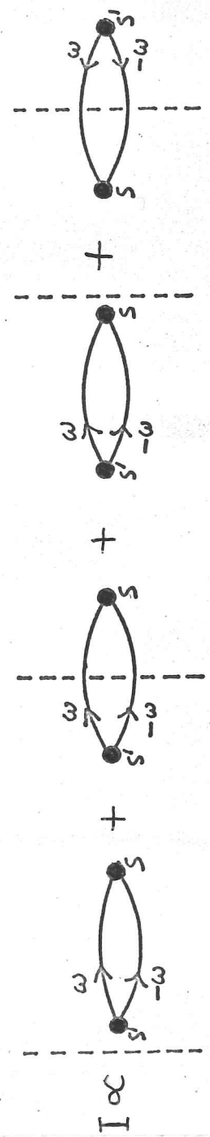

Fig. 18

expression for the current through S contains only Green's functions representing propagation through S (i.e. with s and s' on opposite sides of S). In addition it is gauge-invariant.

The diagram representation and its physical significance

Equation (60) may be given physical significance by representing it by Feynman diagrams (fig. 18). In the diagrams the directed lines represent single-particle Green's functions, one line representing a G function and the other a $\tilde{G}$ function, and they are labelled by the frequency which occurs as a suffix to the Green's function. A dot at a vertex represents a factor Δ^* or Δ according to whether two directed lines emerge from or go into the vertex, and the sum of the frequencies labelling the two lines at a vertex must be zero. The dashed line represents the barrier, and takes into account the factor n(s') - n(s). More precisely, one must multiply each diagram by a factor proportional to the number of electrons which the diagram shows crossing the barrier (i.e. 0, 2, 0, -2 respectively for the diagrams of fig. 18). The quantity which a diagram represents must be integrated with respect to the coordinates of the vertices and summed with respect to frequency in the usual way, and the sum over all diagrams is a quantity proportional to the barrier current. Physically, we may say that the diagrams represent the following process: a Cooper pair scatters at s', propagates to s and then scatters again. If in going from s' to s it crosses the barrier, this process contributes to the barrier supercurrent. From this we see that the existence of an interaction in the barrier

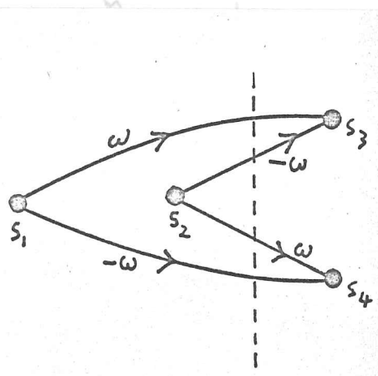

Fig. 19

itself is not a necessary condition for supercurrents to be able to flow through the barrier.

Processes involving more than two Cooper pairs can also occur, and it is these processes which require one of the Green's functions to be a G instead of a $\tilde{G}$. In fact, if an expression for G in terms of $\tilde{G}$, Δ and Δ^* is obtained by iterating (46) and substituted into (60) the resulting expression is represented diagrammatically by an infinite set of connected diagrams, a typical one being that of fig. 19, which represents a process involving four electrons crossing the barrier and four scattering processes involving the superconducting interaction. In these diagrams all directed lines are $\tilde{G}$ functions.

If one examines the foregoing explanation of the processes occurring more closely some rather curious features emerge. For example, Feynman diagrams normally represent probability amplitudes for processes and one would therefore have expected the current through the barrier to have been the square of the modulus of the sum of the Feynman diagrams instead of just the sum. A similar feature has also been noted in previous analyses (Josephson 1962, Ferrell and Prange 1963), and it is responsible for the fact that supercurrents through barriers, which are due to second order processes, are similar in magnitude to the first order quasi-particle processes. Another curious feature is that the contribution to the current from each diagram is in general complex, though the sum is real, as it must be, each diagram having a complex conjugate

diagram obtained from it by reversing all its arrows. It is clear that intuition is of no great help in understanding the supercurrent as a flow of Cooper pairs. However, as will now be shown, there are some very familiar situations in which similar difficulties arise if one tries to interpret them in terms of a flow of particles (for a different example, see Ferrell and Prange 1963).

Consider a charged particle in a harmonic potential well, interacting with an external oscillating electric field. The interaction between the particle and the field may be pictured as follows: the quantum number of the state of the electron may change by ± 1 and a photon be simultaneously absorbed or emitted. The matrix element for these processes is proportional to the electronic charge e, and as shown by standard theory the probability of emission of a photon (in the absence of an applied field) or absorption or stimulated emission (in the presence of a continuous spectrum of electromagnetic radiation) is proportional to the squared matrix element, i.e. to e^2. Now consider instead a <u>coherent</u> applied electromagnetic field oscillating in phase with the electron. If the quantum numbers of the electron and the field are large we may calculate classically the mean rate at which power is transferred from the field to the electron:

$$P = eEv \sin \phi \qquad (61)$$

where E and v are the root mean square values of the electric field and the velocity of the electron respectively and ϕ is the phase difference between the two oscillations. Since the photon energy is fixed, $\dot{n}$, the mean rate at which quanta are transferred from

the field to the electron, is proportional to P and hence to $e \sin \phi$, i.e. proportional to the matrix element and not to its square. It should be noted that the usual perturbation theory treatment for the rate at which a process occurs is not applicable here, since the spectrum of final states is not quasi-continuous as is usually assumed. Note also the appearance in (61) of the factor $\sin \phi$, just as in the case of barriers (equation 9).

At this point we may take a lead from the treatment of barriers and say that there are two contributions to $\dot{n}$, one proportional to $ie \exp(-i\phi)$ from the absorption of photons and one proportional to $-ie \exp(i\phi)$ from the emission of photons. As with other interference processes, any attempt to observe which way any individual process has taken place alters the nature of the effect. To be able to tell whether between two instants of time a photon has been absorbed or emitted it is necessary to know the quantum number of either the electron or the field at both times to better than unity, which destroys knowledge of the phases. Equation (61) has meaning only when averaged over a large number of quantum processes.

Interference effects

After this digression, let us return to the discussion of barriers. In particular we shall consider the question of whether the summations and integrations implied by equation (60) involve quantities which tend to have the same sign (more precisely, whose real parts tend to have the same sign), or whether the signs tend to be random, which will tend to reduce the magnitude of the supercurrents.

In the first place, phase changes may occur in the product

$\Delta(s)\Delta^*(s')$ as s and s' move in a direction parallel to the plane of the barrier. The effect of this on the barrier supercurrent is just the interference effect discussed in section (iv), and the phase changes occur only in the presence of a magnetic field. Then there is the possibility of interference between the two integrals in equation (60). These change relative phase as the phases of Δ on the two sides of the barrier change relative to each other, but this effect merely gives rise to the $\sin\emptyset$ dependence of j_z. Next there is the possibility that Δ may change sign as one moves normal to the barrier, owing to the Coulomb repulsion dominating in the barrier. This effect is probably small for typical tunnelling barriers since their thickness is so small, but it may play an important role in barriers of normal metal. Finally, there is the possibility of fluctuations in sign of $G_{-\omega}(s',s)\tilde{G}_{\omega}(s',s)$. Since Green's functions oscillate in sign with a period of the order of an inverse Fermi wave-number, one might expect this effect to be very important, but we shall see that in the absence of magnetic impurities this is not so. If magnetic fields and impurities are absent then $H_r^* = H_r$, so that by (42)

$$\tilde{G}_{\omega}(s',s) = \{\tilde{G}_{-\omega}(s',s)\}^*$$

In addition G and $\tilde{G}$ are identical at the transition temperature and generally tend to have the same phase (G decreases faster with distance separating the two arguments than $\tilde{G}$). Hence $G_{-\omega}(s',s)\tilde{G}_{\omega}(s',s)$ tends to have the same sign as $|\tilde{G}_{\omega}(s',s)|^2$, which is always positive. Thus non-magnetic impurities should not have a drastic effect on

barrier supercurrents, but with magnetic impurities destructive interference is possible. This distinction between the effects of magnetic and non-magnetic impurities is similar to that occurring in bulk superconductors (Anderson 1959).

To conclude this section, it should be pointed out that the method used here may be generalized in several directions. For example, spin-changing interactions can be dealt with by using a G, $\tilde{G}$ and F^+ which are matrices in the spin indices. Non-local interactions can be dealt with by using a Δ which is a function of two position coordinates instead of one, and retarded interactions by using a Δ which depends on ω. Once the appropriate generalization of the Gor'kov equation has been written down, the subsequent manipulations are essentially identical to those carried out here.

Appendix Calculation of H_{c1}

As pointed out by Abrikosov (1957), the field at which the transition to the mixed state occurs is equal to $4\pi F/\phi_o$, where $\phi_o = hc/2e$ is the flux quantum and F is the free energy of an isolated flux line per unit length. This expression comes from using the equilibrium condition $dF = H\,dM$ (M = magnetization) and the fact that the magnetic moment contributed by unit length of a flux line is $\phi_o/4\pi$.

The free energy of a barrier per unit area is

$$f = \frac{\hbar}{2e} j_1 \left(-\cos\phi + \tfrac{1}{2}\chi^2(\nabla\phi)^2\right) \qquad (62)$$

The first term is that due to the barrier itself, and was derived in section (iii). The second term is the energy of the magnetic field plus the kinetic energy of the supercurrents in the penetration

region. This contribution is clearly proportional to the square of the field in the barrier and so to $(\nabla\phi)^2$, and the coefficient can most simply be found by using the fact that applying the variational principle to the free energy expression obtained from (62) must lead to (16). For the barrier containing no flux line the appropriate solution of (16) is $\phi = 0$, and the solution corresponding to an isolated flux line in the barrier is the one derived by Ferrell and Prange (1963) in a different connection:

$$\phi_f = 2 \sin^{-1} \operatorname{sech} (x/\lambda) \tag{63}$$

which clearly corresponds to a disturbance localized near the line $x = 0$. Substituting into the free energy formula (62), we obtain for the additional energy per unit length of a flux line

$$F = (\hbar j_1/2e)\int_{-\infty}^{\infty} \left\{ (1 - \cos\phi_f) + \tfrac{1}{2}\lambda^2 \left(\frac{d\phi_f}{dx}\right)^2 \right\} dx$$

$$= (2\hbar j_1/e)\int_{-\infty}^{\infty} \operatorname{sech}^2 (x/\lambda)\, dx = (2\hbar j_1 \lambda/e)\int_{-\infty}^{\infty} \operatorname{sech}^2 x\, dx$$

$$= 4\hbar j_1 \lambda/e \tag{64}$$

$$= (2\hbar^3 j_1 c^2/\pi e^3 d)^{\frac{1}{2}} \tag{65}$$

Therefore $H_{c1} = 4\pi F/\left(\frac{hc}{2e}\right)$

$$= (32\ \hbar j_1/\pi e d)^{\frac{1}{2}} \tag{66}$$

REFERENCES

Abrikosov, A. A. (1957), Soviet Phys. JETP, 5, 1174.

Adkins, C. J. (1961), J. Sci. Instr. 38, 305.

Ambegaokar, V. and Baratoff, A. (1963), Phys. Rev. Letters, 10, 486 and 11, 104 (erratum).

Anderson, P. W. (1959), J. Phys. Chem. Solids, 11, 26.

Anderson, P. W. (1962), Phys. Rev. Letters 9, 309.

Anderson, P. W. (1963), Lecture at the Ravello Spring School.

Anderson, P. W. and Rowell, J. M. (1963), Phys. Rev. Letters 10, 230.

Bardeen, J. (1958), Phys. Rev. Letters 1, 399.

Bean, C. P. and Livingston, J. D. (1964), Phys. Rev. Letters 12, 14.

Cohen, M. H., Falicov, L. M. and Phillips, J.C. (1962), Phys. Rev. Letters 8, 316.

Cooper, L. N. (1956), Phys. Rev. 104, 1189.

Dresselhaus, G. and Dresselhaus, M. S. (1960), Phys. Rev. 118, 77 and Phys. Rev. Letters 4, 401.

Eck, R. E., Scalapino, D. J. and Taylor, B. N. (1964), Phys. Rev. Letters 13, 15.

Ehrenberg, W. and Siday, R. E. (1949), Proc. Phys. Soc. (London), B62, 8.

Fawcett, E. (1960), The Fermi Surface, ed. Harrison and Webb, Wiley, N.Y. and London, p. 197.

Ferrell, R. A. and Prange, R. E. (1963), Phys. Rev. Letters 10, 479.*

* Assiduous readers detecting an inconsistency between the declaration made in the first paragraph of the preface and reference 4 of this paper are assured that I have never even set foot in the state of Massachusetts, let alone submitted a Ph. D. thesis to any university there. Also,

(cont.)

Fiske, M.D. (1964), Revs. Mod. Phys. 36, 221.

Ginzburg, V.L. and Landau, L.D. (1950), J. Exptl. Theoret. Phys. (USSR), 20, 1064.

Gor'kov, L.P. (1958), Soviet Phys. JETP 7, 505.

Gor'kov, L.P. (1959), Soviet Phys. JETP 9, 1364.

Gor'kov, L.P. (1960), Soviet Phys, JETP 10, 593.

Gorter, C.J. and Casimir, H.B.G. (1934) Phys. Z. 35, 963 and Z. Techn. Phys. 15, 539.

Jaklevic, R.C., Lambe, J., Silver, A.H. and Mercereau, J.E. (1964), Phys. Rev. Letters 12, 159.

Josephson, B.D. (1962), Phys. Letters 1, 251 (submitted with this dissertation).

Josephson, B.D. (1964), Revs. Mod. Phys. 36, 216 (submitted with this dissertation).

Keller, J.B. and Zumino, B. (1961), Phys. Rev. Letters 7, 164.

Landau, L.D. and Lifshitz, E.N. (1959), Statistical Physics, Pergamon Press, London, (chapter 14).

London, F. and H. (1935), Proc. Roy. Soc. (London) A149, 71 and Physica 2, 341.

Lynton, E.A. (1962), Superconductivity, Methuen, London, (chaps. 5 and 6).

McLean, W.L. (1960), Thesis, Cambridge University, England.

Pippard, A.B. (1947), Proc. Roy. Soc. (London) A191, 370.

Pippard, A.B. (1950), Proc. Roy. Soc. (London) A203, 98 and 210.

Pippard, A.B. (1961), Proc. VIIth Int. Conf. Low Temp. Phys., North Holland Publishing Company, Amsterdam, p. 320.

---

this dissertation has not taken quite so long to prepare that the authors could have had access in June 1963 to a preliminary draft of it.

Preston-Thomas, H. (1949), J. Sci. Instr. 26, 381.

Richards, P.L. (1962), Phys. Rev. 126, 912.

Rowell, J.M. (1963), Phys. Rev. Letters 11, 200.

Schrieffer, J.R., Scalapino, D.J. and Wilkins, J.W. (1963), Phys. Rev. Letters 10, 336.

Shapiro, S. (1963), Phys. Rev. Letters 11, 80.

Shapiro, S., Janus, A.R. and Holly, S. (1964), Revs. Mod. Phys. 36, 223.

Sharvin, Yu.V. and Gantmakher, V.F. (1961), Soviet Phys. JETP 12, 866.

Spiewak, M. (1958), Phys. Rev. Letters 1, 136.

Spiewak, M. (1959), Phys. Rev. 113, 1479.

Tapp, J.S. (1932), Can. J. Res. 6, 584.

Thouless, D.J. (1960), Ann. Phys. (N.Y.) 10, 553.

Tien, P.K. and Gordon, J.P. (1963), Phys. Rev. 129, 647.